J. Fluid Mech. (2020), *vol.* 888, A28. © The Author(s), 2020.
Published by Cambridge University Press
doi:10.1017/jfm.2020.6

Heterogeneous dispersions as microcontinuum fluids

Benjamin E. Dolata[1,2] **and Roseanna N. Zia**[1,†]

[1]Department of Chemical Engineering, Stanford University, Stanford, CA 94305, USA

[2]Robert Frederick Smith School of Chemical and Biomolecular Engineering, Cornell University, Ithaca, NY 14853, USA

(Received 20 August 2019; revised 21 November 2019; accepted 20 December 2019)

We present a non-local 'microcontinuum' constitutive equation describing particle suspensions undergoing heterogeneous flows in the low Stokes and particle Reynolds number regime. Most prior models rely on mesoscale averages of structural dynamics that smear out non-local effects or otherwise place strong restrictions on flow type. We relieve this restriction here by ensemble averaging the exact equations that govern the suspension at the microscale, thereby obtaining explicit structure-property connections. The result is a pointwise, heterogeneous ensemble average of the suspension stress valid for suspended particles of arbitrary shape, size, composition and concentration, as well as arbitrary sources of heterogeneity, including non-uniform shear fields, heterogeneous force fields or spatially varying volume fractions. This non-local model accounts for spatial and temporal variations in the flow structure over arbitrary length and time scales. We express the microcontinuum constitutive equation as a superposition of gradient operators that automatically accounts for flow heterogeneity over any length scale larger than the particle size. Batchelor's result for a homogeneous suspension is recovered in the limit of zero gradients; non-zero gradient terms provide non-local corrections to the average stress and account for statistical heterogeneity in the suspension. We utilize energy methods to compute the influence of these gradient operators on the pointwise-averaged stress tensor, revealing a deep connection to the microhydrodynamics formalism. We apply this general framework to a dilute suspension of spherical particles and show that the resultant constitutive equations are consistent with experimental observations.

Key words: colloids, general fluid mechanics, non-continuum effects

1. Introduction

Formations of channels, bands and vortices of particles in dispersions are prominent motifs in the flow of initially well-dispersed suspensions, with nearly as many mechanistic explanations and models as physical phenomena. Examples include ring formation in rotating cylinders (Tirumkudulu, Mileo & Acrivos 2000), shear banding (Berret 2006), streaming and vortex instabilities during sedimentation (Whitmore 1955; Batchelor & Van Rensburg 1986; Tee *et al.* 2002; Bergougnoux *et al.* 2003),

† Email address for correspondence: rzia@stanford.edu

https://doi.org/10.1017/jfm.2020.6 Published online by Cambridge University Press

shear-induced migration (Leighton & Acrivos 1987), transient vortices in bacterial dispersions (Dombrowski *et al.* 2004) and chaining in electro- and magneto-rheological fluids (Halsey & Toor 1990; Halsey 1992). The ubiquity of such phenomena implies the need for a general framework that can be applied to any heterogeneous flow.

Attempts to model these behaviours using viscometric constitutive equations derived from homogeneous flows, such as simple shear, have been hampered by the presence of mathematical singularities in the solutions. For example, while the model of shear migration in pressure-driven flow developed by Frank *et al.* (2003) successfully predicts particle migration, it produces a discontinuity in the spatial gradients of the volume fraction (i.e. a cusp in the volume fraction profile) at the centreline. This discontinuity is unphysical and is not found in experiments (Koh, Hookham & Leal 1994; Lyon & Leal 1998*a*,*b*; Frank *et al.* 2003). The authors attribute this failure to 'application of the model at an arbitrarily small length scale'. That is, the model neglects non-local behaviours that may serve to smooth discontinuously sharp gradients on small length scales. Another approach employs non-local balance laws that correct for statistical heterogeneity by adding non-local terms either to the constitutive equation or to the equation of motion for the stress. Such methods originated with the study of higher-gradient continua (Eringen 1966; Stokes 1966; Bleustein & Green 1967) and have been used quite successfully to describe shear banding (Dhont 1999; Olmsted 2008; Masselon, Salmon & Colin 2008; Hemingway & Fielding 2018) and swarming in bacterial suspensions (Wolgemuth 2008; Dunkel *et al.* 2013; Słomka & Dunkel 2017). However, it is unclear if these non-local balance laws, which are largely phenomenological in nature, are generally applicable to arbitrary flows.

This ambiguity may be resolved by utilizing pointwise averaging of the underlying micromechanical equations of motion of the suspension to obtain microcontinuum constitutive equations informed by structure-property relations. An ideal heterogeneous-averaging method should automatically account for all internal length scales of the dispersion without foreknowledge of the magnitude or number of such length scales. Lhuillier (1992) demonstrated that traditional volume-averaging methods (Batchelor 1970) as well as their heterogeneous extensions (Anderson & Jackson 1967; Jackson 1997) place severe restrictions on the suspension length scales (by requiring *a priori* selection of an averaging volume that is thence specific to one length scale) and suggested ensemble averaging as an alternative approach. One such family of ensemble-averaging methods, based on linear momentum conservation (Strating 1995; Dhont & Briels 2002), can be used to compute the divergence of the stress tensor, but is limited to rigid particles, does not account for angular momentum conservation and cannot be readily applied to other ensemble-averaged fields of interest such as the average particle velocity. These limitations can be overcome by the phase-averaging method of Zhang & Prosperetti (1994*a*, 1997), which, in principle, can be used to compute the ensemble average of any field in a suspension of arbitrary composition. However, their methods require the use of high-rank tensors, and hence have largely been limited to dilute suspensions of inviscid spherical droplets (Zhang & Prosperetti 1994*b*) or rigid, solid spheres (Zhang & Prosperetti 1997; Prosperetti 2004; Prosperetti, Zhang & Ichiki 2006) due to the mathematical complexity involved in separating field averages in the fluid from those in the particles, which are most tractable as moments of the hydrodynamic surface traction.

The primary outcome of the present work is a framework for computing the stress tensor as a pointwise average in heterogeneous dispersions of particles of arbitrary

https://doi.org/10.1017/jfm.2020.6 Published online by Cambridge University Press

shape and composition, valid for arbitrary spatial and temporal variations in flow structure. To reveal how heterogeneity enters the stress via velocity and concentration gradients, we show that the particle-phase stress can also be expressed as a series expansion accounting for non-local correlations between nearby material points. To overcome the challenges associated with particle field averaging, we recognize that the energy methods contains symmetries that encode the dynamically relevant tensorial structure of the general solution. We use this general structure to re-express the stress moments as moments of the hydrodynamic traction and fluid velocity on the particle surface.

The remainder of the paper is organized as follows. In § 2, a non-local integral constitutive equation for the stress tensor in a heterogeneous dispersion is derived. Following Lhuillier (1992), this integral equation is rewritten as a moment expansion of the stress interior to the particle to facilitate its evaluation. The physical relevance of these moments to heterogeneous flow are discussed. Recognizing a connection to microhydrodynamics, in § 3, the volume integrals are converted into surface integrals in order to apply the mathematical methods of microhydrodynamics to the dispersion; we next show that the moments can be expressed in terms of a grand resistance matrix coupling fluid/surface traction to velocity derivatives. In § 4, the framework is applied to a dilute suspension of spheres of arbitrary composition. General constitutive equations independent of the material composition of the particles are obtained. To validate the model, we apply it to the case of viscous droplets and Navier-slip spheres. The results correct and extend several prior results for constitutive equations of rigid spheres (Einstein 1906, 1911; Prosperetti 2004; Prosperetti *et al.* 2006; Jin *et al.* 2018; Zhou & Prosperetti 2020) and viscous droplets (Taylor 1932; Raja, Subramanian & Koch 2010), and are shown to be consistent with experimental observations. The study is concluded with a discussion of results and future prospects.

2. Heterogeneous average of the stress

In this section, a method is developed to compute the average stress in heterogeneous suspensions. This study is inspired by the pioneering work of Zhang & Prosperetti (1994*a*, 1997) towards development of 'phase-averaging' techniques to describe multiphase flows. We describe such suspensions mathematically as a statistically non-uniform N-particle ensemble; no restrictions are placed on the number, shape or compositions of the particles. The most general expression for the ensemble average of the stress σ_{ij} at any material point x_i in a suspension is

$$\langle\sigma_{ij}\rangle(\boldsymbol{x}) = \int \sigma_{ij}(\boldsymbol{x}|\mathscr{C})P(\mathscr{C})\,\mathrm{d}\mathscr{C}, \tag{2.1}$$

where $P(\mathscr{C})$ is the probability of finding the system at a configuration $\mathscr{C}$ in the phase space of all degrees of freedom in the suspension. The probability density function should be understood as an implicit function of time: $P(\mathscr{C}) \equiv P(\mathscr{C}, t)$. In the interest of mathematical simplicity, we will, without loss of generality, neglect explicit treatment of the time evolution of the averages.

The primary difficulty encountered in the ensemble averaging of colloidal dispersions arises from the need to incorporate and track the location of particle/fluid interfaces throughout the averaging process. Zhang & Prosperetti (1994*a*, 1997) demonstrated that interfaces can be naturally accounted for utilizing a characteristic function $\chi(\boldsymbol{x}|\mathscr{C})$, defined as $\chi = 1$ when x_i is located in the fluid and $\chi = 0$ when x_i

https://doi.org/10.1017/jfm.2020.6 Published online by Cambridge University Press

is inside a particle, which splits the ensemble average of any field into the sum of a fluid-phase average and particle-phase average. Utilizing this characteristic function, the ensemble-averaged stress becomes (Prosperetti 2004; Prosperetti *et al.* 2006)

$$\langle \sigma_{ij} \rangle (\boldsymbol{x}) = \langle \chi \sigma_{ij}^{f} \rangle (\boldsymbol{x}) + \langle (1-\chi) \sigma_{ij}^{p} \rangle (\boldsymbol{x}), \tag{2.2}$$

where the superscripts f and p represent the fluid and particle phases, respectively. We assume the suspending liquid is Newtonian with viscosity η, with the fluid stress constitutively specified as

$$\sigma_{ij}^{f} = -p^{f} \delta_{ij} + 2\eta e_{ij}^{f}, \tag{2.3}$$

where p is the thermodynamic pressure, $e_{ij} = u_{\{i,j\}}$ is the shear-rate tensor and u_i is the velocity field. Substituting (2.3) into (2.2) yields

$$\langle \sigma_{ij} \rangle = -\langle \chi p^{f} \rangle \delta_{ij} + 2\eta \langle \chi e_{ij}^{f} \rangle + \langle (1-\chi) \sigma_{ij}^{p} \rangle. \tag{2.4}$$

Our point of departure from the method of Zhang & Prosperetti (1994*a*, 1997) is our treatment the fluid- and particle-phase averages. Inspired by Batchelor (1970), we seek to convert the fluid-phase average into an average over the entire suspension. This is for both practical and heuristic reasons: measuring the stress in only the fluid phase would be difficult. Moreover, we are not interested in the stress inside the particles, but rather the additional stress arising from their presence in the fluid. Conversion to a suspension average is accomplished by extending the fluid-phase averages to the particle phase,

$$\begin{aligned} \langle \sigma_{ij} \rangle \;=\; & -\langle \chi p^{f} \rangle \delta_{ij} + 2\eta \langle \chi e_{ij}^{f} \rangle + \langle (1-\chi)(-p^{p} \delta_{ij} + 2\eta e_{ij}^{p}) \rangle \\ & + \langle (1-\chi) \sigma_{ij}^{p} \rangle - \langle (1-\chi)(-p^{p} \delta_{ij} + 2\eta e_{ij}^{p}) \rangle. \end{aligned}$$

This yields, with suspension averages denoted by removing superscripts,

$$\langle \sigma_{ij} \rangle = -\langle p \rangle \delta_{ij} + 2\eta \langle e_{ij} \rangle + \langle (1-\chi) \Sigma_{ij} \rangle, \tag{2.5}$$

where the particle stress

$$\Sigma_{ij} = \sigma_{ij}^{p} + \delta_{ij} p^{p} - 2\eta e_{ij}^{p} \tag{2.6}$$

is the difference between the stress inside the particle, σ_{ij}^{p}, and the stress that would arise if the particle were replaced by pure solvent. This definition has two advantages when compared to prior definitions where the particle stress is simply defined as the average of the stress inside the particle (Prosperetti 2004; Prosperetti *et al.* 2006). First, this quantity is identically zero for all points except those inside the particle and those bounded by the ϵ-thin interfaces between the continuous and dispersed phase. Second, this quantity is amenable to transformation from the particle volume to its surface, where information is more readily available, allowing for the development of fundamental connections between heterogeneous flow problems and the mathematical framework of microhydrodynamics, as will be shown in § 3.

Explicit evaluation of (2.5) requires enumeration of the degrees of freedom contained in $\mathscr{C}$. Zhang & Prosperetti (1994*a*, 1997) demonstrated that the phase space of an N-particle heterogeneous dispersion of spherical particles is given by the position y_i^{α} and velocity U_i^{α} of each particle α. Here, we will extend this result by

https://doi.org/10.1017/jfm.2020.6 Published online by Cambridge University Press

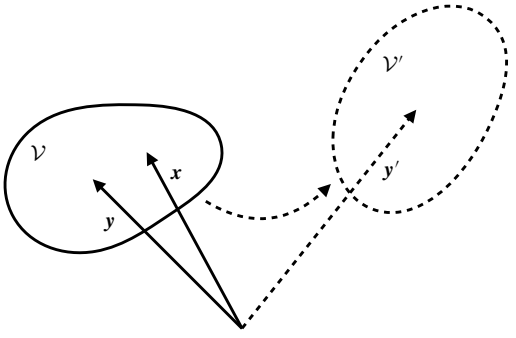


FIGURE 1. A particle moves from $\boldsymbol{y}$ and $\mathcal{V}$ to $\boldsymbol{y}'$ and $\mathcal{V}'$ in position and shape space by translation and deformation, while the material point $\boldsymbol{x}$ remains fixed.

considering a suspension of N particles of arbitrary shape, size and concentration. To this end, we describe the geometric degrees of freedom of the particle with a generic shape parameter $\mathcal{V}_p^\alpha$, which gives the set of all points bounded by S_p^α, the surface of particle α, in addition to the position y_i^α. In the interest of mathematical simplicity we will consider the overdamped limit, where the velocity of the particle and its surface are not independent degrees of freedom. Relaxing this assumption would leave the averaging method essentially unchanged.

As illustrated in figure 1, particles move through y_i space by translation and through $\mathcal{V}_p$ space by rotation and deformation. This framework naturally accounts for the possibility of polydispersity in the suspension. For instance, rigid spheres of different size can be viewed as generic particles held fixed at different points in $\mathcal{V}_p$ space. For mathematical simplicity, it is assumed that each particle in the suspension is of identical material composition. This assumption is not essential to the results presented here, and is easily relaxed.

Because the particle stress (2.6) vanishes when x_i is in the fluid, only configurations where x_i is located in the particle, i.e. where $\boldsymbol{x} - \boldsymbol{y}^\alpha \in \mathcal{V}_p^\alpha$, contribute to the heterogeneous averages, yielding,

$$\langle (1-\chi)\,\Sigma_{ij}\rangle = \sum_\alpha \int \int_{\boldsymbol{x}-\boldsymbol{y}^\alpha \in \mathcal{V}_p^\alpha} P(\boldsymbol{y}^\alpha, \mathcal{V}_p^\alpha)\langle \Sigma_{ij}\rangle(\boldsymbol{x}|\boldsymbol{y}^\alpha, \mathcal{V}_p^\alpha)\,\mathrm{d}\boldsymbol{y}^\alpha\,\mathrm{d}\mathcal{V}_p^\alpha, \tag{2.7}$$

where $P(\boldsymbol{y}^\alpha, \mathcal{V}_p^\alpha)$ is the probability that particle α is located at position y_i^α with shape $\mathcal{V}_p^\alpha$ and $\langle \Sigma_{ij}\rangle(\boldsymbol{x}|\boldsymbol{y}^\alpha, \mathcal{V}_p^\alpha)$ is the conditional average of Σ_{ij} over the remainder of the configuration space $\mathscr{C}$ given that y_i^α and $\mathcal{V}_p^\alpha$ are fixed. Computation of this conditional average is an $(N-1)$-body problem with a solution that depends on the concentration and shape of the particles as well as properties of the flow. Noting that a particle with shape $\mathcal{V}_p$ located at a position y_i is indistinguishable from any other particle with the same position and shape, equation (2.7) can be recast as

$$\langle (1-\chi)\,\Sigma_{ij}\rangle = \int \int_{\boldsymbol{x}-\boldsymbol{y}\in \mathcal{V}_p} n(\boldsymbol{y})\langle \Sigma_{ij}\rangle(\boldsymbol{x}|\boldsymbol{y}, \mathcal{V}_p)P(\mathcal{V}_p|\boldsymbol{y})\,\mathrm{d}\boldsymbol{y}\,\mathrm{d}\mathcal{V}_p, \tag{2.8}$$

where n is the number density and $P(\mathcal{V}_p|\boldsymbol{y})$ is the probability that a particle located at y_i will have shape $\mathcal{V}_p$.

https://doi.org/10.1017/jfm.2020.6 Published online by Cambridge University Press

The expression for the particle stress derived in (2.8) is a non-local constitutive equation and is formally exact, but in practice is difficult to evaluate. Integration of (2.8) requires knowledge of the value of Σ_{ij} at a fixed material point x_i as the particle position y_i is varied. However, integrals over material space are easier to manipulate because differential identities in material space may be derived using continuum balance laws, whereas identities in configuration space require manipulation of a Fokker–Planck equation. This suggests the potential convenience of recasting the configuration space integral as a material space integral. Lhuillier (1992) demonstrated that configuration space particle-phase averages can be recast as integration in physical space through a Taylor series expansion of the integrand. Writing the average stress as

$$\langle (1-\chi)\Sigma_{ij}\rangle = \int \langle (1-\chi)\Sigma_{ij}\rangle(\boldsymbol{\xi})\delta(\boldsymbol{x}-\boldsymbol{\xi})\,\mathrm{d}\boldsymbol{\xi},$$

and Taylor expanding the Dirac delta function about $\xi_i = y_i$ yields a material space average,

$$\langle \Sigma_{ij}\rangle(\boldsymbol{x}) = n(\boldsymbol{x})\langle D_{ij}\rangle(\boldsymbol{x}) - \frac{\partial}{\partial x_k} n(\boldsymbol{x})\langle Q_{ijk}\rangle(\boldsymbol{x}) + \frac{\partial^2}{\partial x_\ell \partial x_k} n(\boldsymbol{x})\langle O_{ijk\ell}\rangle(\boldsymbol{x}) + \cdots, \tag{2.9}$$

where

$$D_{ij} = \int_{\mathcal{V}_p} (\sigma^p_{ij} + p^p\delta_{ij} - 2\eta e^p_{ij})\,\mathrm{d}V, \tag{2.10}$$

$$Q_{ijk} = \int_{\mathcal{V}_p} (\sigma^p_{ij} + p^p\delta_{ij} - 2\eta e^p_{ij}) r_k\,\mathrm{d}V, \tag{2.11}$$

$$O_{ijk\ell} = \tfrac{1}{2}\int_{\mathcal{V}_p} (\sigma^p_{ij} + p^p\delta_{ij} - 2\eta e^p_{ij}) r_k r_\ell\,\mathrm{d}V, \tag{2.12}$$

are the dipole, quadrupole and octupole moments of the stress in the particle, respectively, for a particle located at x_i, and $r_i = x_i - y_i$. The Taylor expansion corresponds to a small wavenumber expansion of the non-local constitutive equation (2.5), which will uniformly converge to the exact expression provided the macroscopic length scale over which the stress varies is larger than the particle size. The gradients of these moments provide non-local corrections to the stress arising from heterogeneity, providing a smoothly varying average between regions of different statistical properties. Higher degrees of accuracy can be obtained by including additional multipole moments after the octupole, with a commensurate increase in mathematical complexity. However, as we will show, truncating at the octupole moment typically provides sufficient accuracy for most physical systems.

3. Evaluation of the multipole moments

The multipole moments defined in (2.10)–(2.12) are volume integrals over the particle interior and the particle/fluid interfacial layer; these integrals cannot be directly evaluated in many cases due to indeterminacies in the stress in the particle interior or in the interface. For instance, the surface tension in droplets leads to an indeterminacy in the interfacial stress analogous to the indeterminacy of the pressure in incompressible fluids. This indeterminacy may be resolved by expressing

https://doi.org/10.1017/jfm.2020.6 Published online by Cambridge University Press

the volume integrals of the stress and shear rate in terms of surface integrals of the hydrodynamic stress and velocity located just outside the interface. In this section, the conservation laws of linear and angular momentum in the particle phase presented in § 3.1 will be combined with energy methods in § 3.2 to extract tensorial symmetries that allow expression of the volume integrals as surface integrals.

3.1. *Conservation laws*

Conversion of the multipole moments D_{ij}, Q_{ijk} and $O_{ijk\ell}$ into surface integrals is facilitated by enforcing conservation laws that can be used to derive differential identities. Expressing all information about the particle phase in terms of balance equations, rather than by constitutive equations, will avoid making unnecessarily restrictive assumptions. We first enforce conservation of momentum on the fluid phase; colloidal particles are small, so inertia is negligible on the particle scale and fluid motion is governed by the Stokes equations

$$-p_{,i} + \eta u_{i,jj} = 0, \tag{3.1a}$$

$$u_{i,i} = 0. \tag{3.1b}$$

Partial differentiation is denoted with commas as $a_{,i} = \partial_i a = \partial a/\partial x_i$.

Solution of the Stokes equations in a dispersion is an inherently many-body problem requiring a closure relation for analytical treatment. A physically motivated closure relation is obtained by noting that the number of particles located a distance r from a test particle is $O(\phi r^2)$, where ϕ is the volume fraction. As $r \to \infty$, the number of particles become large and their combined behaviour tends towards their average,

$$u_i \to \langle u_i \rangle \quad \text{as } r \to \infty. \tag{3.2}$$

This closure relation introduces mathematical inconsistencies that manifest as divergent integrals when computing suspension properties (Batchelor 1972; Batchelor & Green 1972*b*; Jeffrey 1973). The general approach to resolving this problem is to recast either the equations of motion or the boundary conditions in a self-consistent way by e.g. using a renormalization procedure (O'Brien 1979). The motion of the fluid is set by motion of the boundaries, which can also be described by enforcing conservation of momentum, but now on the particle phase.

Particle velocity can arise in two ways. First, particles may be acted on by a body-force density f_i and or a body-torque density l_i, so that conservation of linear and angular momentum in the particle phase is given by

$$\sigma^p_{ij,j} + f_i = 0, \tag{3.3a}$$

$$\varepsilon_{ijk}\sigma^p_{kj} + l_i = 0. \tag{3.3b}$$

These expressions neglect the potential presence of dipolar or couple stresses (cf. Eringen 1966; Stokes 1966; Bleustein & Green 1967) arising from heterogeneity interior to the particle. However, such stresses can be safely neglected unless the particle itself is constructed from a highly heterogeneous medium (Grad 1952; Maranganti & Sharma 2007). Second, continuity of traction and velocity across the interface

$$\sigma^f_{ij} n_j = \sigma^p_{ij} n_j \quad \text{on } S_p, \tag{3.4a}$$

$$u^f_i = u^p_i \quad \text{on } S_p, \tag{3.4b}$$

https://doi.org/10.1017/jfm.2020.6 Published online by Cambridge University Press

can result in momentum transport between the fluid and particle. That is, flow can carry a particle along. Note that the traction and velocity may jump across the interface in the general case. However, explicit inclusion of interfacial balance laws demonstrates that the jump condition plays no role in the suspension rheology (Nadim 1996) and continuity across the interface may be assumed with no loss of generality in the formulation of surface integrals. Finally, the conversion of volume integrals of the stress moments into surface integrals will by greatly facilitated by assuming the particles are incompressible

$$u^p_{i,i} = 0. \tag{3.5}$$

In principle, this assumption could be relaxed by employing the theoretical methods of compressible, low Reynolds number flow (Parmar, Haselbacher & Balachandar 2012).

3.2. *Conversion to surface integrals*

The goal of this section is to express the multipole moments D_{ij}, Q_{ijk} and $O_{ijk\ell}$ in terms of four tensor types,

$$F^{(H,n)}_{ij_1\ldots j_n} = \int_{S_p} \sigma^f_{ik} n_k r_{j_1} \ldots r_{j_n}\, \mathrm{d}S, \tag{3.6a}$$

$$F^{(b,n)}_{ij_1\ldots j_n} = \int_{\mathcal{V}_p} f_i r_{j_1} \ldots r_{j_n}\, \mathrm{d}V, \tag{3.6b}$$

$$V^{(n)}_{ij_1\ldots j_n} = \int_{S_p} u^f_i n_{j_1} r_{j_2} \ldots r_{j_n}\, \mathrm{d}S, \tag{3.6c}$$

$$L^{(n)}_{ij_1\ldots j_n} = \int_{\mathcal{V}_p} l_i r_{j_1} \ldots r_{j_n}\, \mathrm{d}V, \tag{3.6d}$$

which are the nth surface traction moment, the nth body force moment, the nth velocity moment and the nth body torque moment, respectively. The superscripts H and b indicate hydrodynamic and body-force moments, respectively. These tensors can be computed exactly provided that the fluid velocity, surface traction, body forces and torques acting on the particles are known, resolving any indeterminacies associated with interfacial stresses (cf. § 3).

The angular momentum balance (cf. (3.3*b*)) reveals that the antisymmetric part of the stress tensor may be expressed in terms of the torque pseudo-vector

$$\sigma^p_{[ij]} = \tfrac{1}{2}\varepsilon_{ijk} l_k,$$

where we denote antisymmetrization of the enclosed indices with square braces, from which it follows that the portion of the multipole moments D_{ij}, Q_{ijk} and $O_{ijk\ell}$ antisymmetric in i and j can be expressed in terms of the torque moments $\boldsymbol{L}^{(n)}$. The remaining portions of multipole moments, those symmetric in i and j, can be obtained by utilizing the linear momentum balance (cf. (3.3*a*)) to derive differential identities relating the multipole moments to the tensors defined in (3.6). We will obtain such identities using energy methods.

From appendix A, the increase in the rate of work arising from the addition of particles to the fluid is given by,

$$\int_{S_p} (\langle u_i\rangle - U_i - \varepsilon_{i\ell m}\Omega_\ell r_m)\sigma_{ij} n_j\, \mathrm{d}S - \int_{S_p} (\langle \sigma_{ij}\rangle - \langle \Sigma_{ij}\rangle) n_j u^f_i\, \mathrm{d}S, \tag{3.7}$$

https://doi.org/10.1017/jfm.2020.6 Published online by Cambridge University Press

which upon application of the divergence theorem, combined with (3.3*a*) and the boundary conditions (3.4*a*)–(3.4*b*), yields

$$\int_{\mathcal{V}_p} (\langle u_{i,j}\rangle + \varepsilon_{ijk}\Omega_k)\sigma_{ij}^p \,\mathrm{d}V - \int_{\mathcal{V}_p} (\langle \sigma_{ij}\rangle - \langle \Sigma_{ij}\rangle) u_{i,j}^p \,\mathrm{d}V - \int_{V_p} (\langle u_i\rangle - U_i - \varepsilon_{ijk}\Omega_j r_k) f_i \,\mathrm{d}V. \tag{3.8}$$

Substituting the average stress (2.5) into (3.8), equating the resultant expression with (3.7) and rearranging yields

$$\begin{aligned}
&\int_{\mathcal{V}_p} \langle e_{ij}\rangle(\sigma_{ij}^p - 2\eta e_{ij}^p)\,\mathrm{d}V + \int_{\mathcal{V}_p} (\langle u_{[i,j]}\rangle + \varepsilon_{ijk}\Omega_k)\sigma_{ij}^p \,\mathrm{d}V \\
&\quad = \int_{S_p} (\langle u_i\rangle - U_i - \varepsilon_{i\ell m}\Omega_\ell r_m)\sigma_{ij}^f n_j \,\mathrm{d}S + \int_{\mathcal{V}_p} (\langle u_i\rangle - U_i - \varepsilon_{ijk}\Omega_j r_k) f_i \,\mathrm{d}V \\
&\qquad - \int_{S_p} (\langle \sigma_{ij}\rangle - \langle \Sigma_{ij}\rangle) n_j u_i^f \,\mathrm{d}S.
\end{aligned} \tag{3.9}$$

This gives an expression relating the stress and shear-rate fields interior to the particle with the surface traction and velocity, and is exact for all particles governed by the general conditions of § 3.1. A discussion of the relation between the body-force integral in (3.9) and conservative interparticle forces described by interaction potentials is given in B. E. Dolata and R. N. Zia (personal communication 2019). Note that here, as in § 3.1, we assume that there are no body forces acting on the fluid. Body forces localized near particle surfaces such as those arising from electric double layers, may readily be included in an extended definition of the particle pressure, permitting derivation of heterogeneous analogous of the electroviscous effect. In the presence of macroscopic applied fields, such those in electrophoresis, it may prove convenient to treat the stresses induced by these fields as quantities unrelated to the particle stress, by e.g. applying our ensemble-averaging technique to the Maxwell stress tensor.

The averaged fields in (3.9) are spatially varying tensor fields evaluated in the particle interior and at the particle surface. Inspection of the first volume integral on the left-hand side of (3.9) reveals that Taylor expanding these terms about the particle centre will yield terms matching those in in the definitions of the multipole moments (cf. (2.10)–(2.12)). We begin by Taylor expanding the pointwise-averaged velocity field, which, using the identity $u_{i,jk} = 2e_{i(j,k)} - e_{jk,i}$, yields,

$$\begin{aligned}
\langle u_i\rangle(\boldsymbol{x}) - U_i - \varepsilon_{ijk}\Omega_j r_k \;=\; &\langle u_i\rangle(\boldsymbol{y}) - U_i + r_j\langle \gamma_{ij}\rangle(\boldsymbol{y}) + \tfrac{1}{2} r_j r_k (2\langle e_{i(j,k)}\rangle(\boldsymbol{y}) - \langle e_{jk,i}\rangle(\boldsymbol{y})) \\
&+ \tfrac{1}{6} r_j r_k r_\ell (2\langle e_{i(j,k)\ell}\rangle(\boldsymbol{y}) - \langle e_{jk,i\ell}\rangle(\boldsymbol{y})),
\end{aligned} \tag{3.10}$$

where parentheses indicate symmetrization of the enclosed indices and where

$$\gamma_{ij} = u_{i,j} + \varepsilon_{ijk}\Omega_k \tag{3.11}$$

is the relative deformation rate tensor. Next, we obtain an expression for ensemble-averaged stress, which may be obtained from a direct Taylor expansion of (2.1), yielding

$$\begin{aligned}
\langle \sigma_{ij}\rangle - \langle \Sigma_{ij}\rangle \;=\; &2\eta\langle e_{ij}\rangle(\boldsymbol{y}) + 2\eta r_k\langle e_{ij,k}\rangle(\boldsymbol{y}) + \eta r_k r_\ell \langle e_{ij,k\ell}\rangle(\boldsymbol{y}) \\
&- \delta_{ij} r_k \langle p_{,k}\rangle(\boldsymbol{y}) - \tfrac{1}{2}\delta_{ij} r_k r_\ell \langle p_{,k\ell}\rangle(\boldsymbol{y}),
\end{aligned}$$

where we have set the pressure at the particle centre to zero. We assume the average pressure gradient is given by solutions of the Stokes equations $p_{,i} = \eta u_{i,jj} = 2e_{ij,j}$; the consequence of this assumption is discussed in appendix C. Substituting the Stokesian

https://doi.org/10.1017/jfm.2020.6 Published online by Cambridge University Press

pressure yields

$$\begin{aligned}\langle\sigma_{ij}\rangle - \langle\Sigma_{ij}\rangle \;=\; & 2\eta\langle\gamma_{(ij)}\rangle(\boldsymbol{y}) + 2\eta r_k(\langle e_{ij,k}\rangle(\boldsymbol{y}) - \delta_{ij}\langle e_{k\ell,\ell}\rangle(\boldsymbol{y})) \\ & + \eta r_k r_\ell(\langle e_{ij,k\ell}\rangle(\boldsymbol{y}) - \delta_{ij}\langle e_{km,m\ell}\rangle(\boldsymbol{y})),\end{aligned} \tag{3.12}$$

where $\gamma_{(ij)} = e_{ij}$. We then substitute (3.10) and (3.12) into (3.9), yielding the algebraic expressions,

$$F_i^{(H,0)}(\langle u_i'\rangle - U_i) = -F_i^{(b,0)}(\langle u_i\rangle - U_i), \tag{3.13a}$$

$$D_{ij}\langle\gamma_{ij}\rangle = (F_{ij}^{(H,1)} - 2\eta V_{(ij)}^{(1)} + F_{ij}^{(b,1)})\langle\gamma_{ij}\rangle, \tag{3.13b}$$

$$\begin{aligned}Q_{ijk}\langle e_{ij,k}\rangle \;=\; & (\tfrac{1}{2}(2F_{(ij)k}^{(H,2)} - F_{kij}^{(H,2)}) + \tfrac{1}{2}(2F_{(ij)k}^{(b,2)} - F_{kij}^{(b,2)}) \\ & - \varepsilon_{jk\ell}L_{\ell i}^{(1)} - 2\eta(V_{ijk}^{(2)} - \delta_{jk}V_{\ell\ell i}^{(2)}))\langle e_{ij,k}\rangle,\end{aligned} \tag{3.13c}$$

$$\begin{aligned}O_{ijk\ell}\langle e_{ij,k\ell}\rangle \;=\; & (\tfrac{1}{6}(2F_{(ij)k\ell}^{(H,3)} - F_{k\ell ij}^{(H,3)}) + \tfrac{1}{6}(2F_{(ij)k\ell}^{(b,3)} - F_{k\ell ij}^{(b,3)}) \\ & - \tfrac{1}{2}\varepsilon_{jkm}L_{mi\ell}^{(2)} - \eta(V_{ijk\ell}^{(3)} - \delta_{jk}V_{mmi\ell}^{(3)}))\langle e_{ij,k\ell}\rangle.\end{aligned} \tag{3.13d}$$

The relations above hold for every value of $\langle u_i\rangle$, $\langle\gamma_{ij}\rangle$, $\langle e_{ij,k}\rangle$ and $\langle e_{ij,k\ell}\rangle$ consistent with the pointwise-averaged Cauchy momentum equation, conveniently allowing direct recovery of the hydrodynamic force from (3.13*a*) which balances the body force for inertia-free particles,

$$F_i^H = F_i^{(H,0)}. \tag{3.14}$$

The higher-order moments contain indeterminacies associated with index symmetries of the velocity. These indeterminacies arise directly from the governing equations, as follows. First, the pressure field is indeterminate in incompressible flow and serves as a Lagrange multiplier to enforce incompressibility. Thus, individual sources of isotropic stresses (thermodynamic and mechanical) cannot be distinguished and may be combined into a redefined indeterminate spherical stress that enforces incompressibility. Thus, while the gradient of the pressure may be computed and is completely determined by flow boundary conditions, the trace of the stress tensor can take on an infinite number of values. Second, the averaging method itself results in inherent indeterminacies because the multipole moments defined in (2.10)–(2.12) are only unique to within arbitrary solenoidal tensor fields that vanish under the divergence operators in (2.9). This is simply a higher-rank analogue of the indeterminacy associated with the scalar pressure.

The indeterminacy of the pressure is reflected in (3.13*b*), where, because γ_{ij} is traceless, D_{ii}^H can take any value and still satisfy (3.13*b*). The trace of the dipole moment is dynamically insignificant because it may be included as part of an indeterminate spherical pressure, allowing us to make the convenient choice of setting the trace to zero,

$$D_{ij} = F_{ij}^{(H,1)} - \tfrac{1}{3}\delta_{ij}F_{kk}^{(H,1)} - 2\eta V_{(ij)}^{(1)} + F_{ij}^{(b,1)} - \tfrac{1}{3}\delta_{ij}F_{kk}^{(b,1)}, \tag{3.15}$$

yielding a tensor with 8 independent scalar components. The familiar definitions of the stresslet and hydrodynamic torque are the symmetric and antisymmetric parts of the dipole moment, respectively,

$$D_{ij} = S_{ij} - \tfrac{1}{2}\varepsilon_{ijk}L_k^H.$$

https://doi.org/10.1017/jfm.2020.6 Published online by Cambridge University Press

Next, we examine Q_{ijk}. Upon noting that $e_{ij,k}$ is symmetric and traceless in the first two indices, application of the same argument regarding the arbitrary value of the trace yields,

$$\begin{aligned} Q_{ijk} \;=\; & F^{(H,2)}_{\{ij\}k} - \tfrac{1}{2}F^{(H,2)}_{k\{ij\}} - \eta(2V^{(2)}_{(ij)k} - \delta_{ik}V^{(2)}_{\ell\ell j} - \delta_{jk}V^{(2)}_{\ell\ell i}) \\ & + F^{(b,2)}_{\{ij\}k} - \tfrac{1}{2}F^{(b,2)}_{k\{ij\}} - \Delta^{(2,2)}_{ijmp}\varepsilon_{mk\ell}L^{(1)}_{\ell p} + \tfrac{1}{2}\varepsilon_{ij\ell}L^{(1)}_{\ell k}, \end{aligned} \tag{3.16}$$

after symmetrizing the quadrupole and rendering the first two indices traceless, and adding the antisymmetric component arising from the torque balance. Indices enclosed in curly braces have been made symmetric and traceless. We may divide the quadrupole moment into a hydrodynamic quadrupole Q^H_{ijk} dependent on the hydrodynamic traction and fluid velocity and a non-hydrodynamic portion dependent on body forces and torques; the hydrodynamic quadrupole is a tensor with 15 independent components.

The process of constructing the octupole moment is more involved. Whereas indeterminacies in D^H_{ij} and Q^H_{ijk} were resolved by removing the trace, the two divergence operators acting on $O_{ijk\ell}$ in (2.9) yield a larger freedom of choice in resolving the indeterminacies of the octupole moment. As outlined in appendix C, removing these indeterminacies gives the octupole moment as the sum of the hydrodynamic octupole moment with (which contains 24 independent components) and moments of the body forces and torques,

$$\begin{aligned} O^H_{ijk\ell} \;=\; & \mathscr{P}_{ijk\ell mpqr}(\tfrac{1}{6}(2F^{(H,3)}_{(mp)qr} - F^{(H,3)}_{qrmp}) - \eta(V^{(3)}_{mpqr} - \delta_{pq}V^{(3)}_{ssmr})) \\ & + 2\Delta^{(2,1,2)}_{ijmpk\ell}\int_{\mathcal{V}_p} r_m u_p \,\mathrm{d}V \\ & + \mathscr{P}_{ijk\ell mpqr}(\tfrac{1}{6}(2F^{(b,3)}_{\{mp\}qr} - F^{(b,3)}_{qr\{mp\}}) - \tfrac{1}{2}\varepsilon_{mqs}L^{(2)}_{spr}) + \tfrac{1}{4}\varepsilon_{ijm}L^{(2)}_{mk\ell}, \end{aligned} \tag{3.17}$$

where

$$\begin{aligned} \mathscr{P}_{ijk\ell mpqr} \;=\; & \tfrac{1}{2}\Delta^{(2,2)}_{ijmp}(\delta_{kq}\delta_{\ell r} + \delta_{kr}\delta_{\ell q}) - \tfrac{1}{5}\Delta^{(2,2)}_{ijk\ell}\Delta^{(2,2)}_{mpqr} \\ & - \tfrac{75}{8}(\Delta^{(3,3)}_{ij(k\ell)no} - \tfrac{8}{15}\Delta^{(2,2)}_{ijno}\delta_{k\ell})(\tfrac{8}{7}\Delta^{(3,3)}_{mp(qr)no} - \tfrac{8}{15}\Delta^{(2,2)}_{mpno}\delta_{qr}) \end{aligned}$$

and we have added the antisymmetric component dependent on the body torques. Here, we define the tensor operator $\Delta^{(n,n)}_{i_1\ldots i_n j_1\ldots j_n}$ as the projector of a rank-n tensor onto the subspace of rank-n harmonic tensors (symmetric and traceless in all indices) (Ehrentraut & Muschik 1998), $\mathscr{E}^{(n,n)}_{i_1\ldots i_n j_1\ldots j_n}$ as the generalized Kronecker delta that projects a rank-n tensor onto a completely antisymmetric tensor (Agacy 1999) and $\Delta^{(2,1,2)}_{ijk\ell mp}$ is a Clebsch–Gordan tensor (Coope 1970) which gives the irreducible rank-two product of an antisymmetric tensor (i.e. a pseudovector) and an irreducible second-rank tensor. The functional forms of the operators may be found in appendix B.

The first term in this operator $\mathscr{P}_{ijk\ell mpqr}$ projects the octupole moment onto the correct index symmetries, while the other two terms serve to remove dynamically indeterminate parts of the stress. Note that there is a remainder velocity volume integral in the octupole which cannot be expressed as a surface integral. This term, as discussed in appendix C, is indeterminate in the Stokes equations, but may have dynamic significance in general heterogeneous flows. This remainder cannot generally be evaluated directly, but may be computed indirectly using generalized Faxén laws

https://doi.org/10.1017/jfm.2020.6 Published online by Cambridge University Press

(B. E. Dolata and R. N. Zia, personal communication 2019) and the Lorentz reciprocal theorem. We have thus obtained all multipole moments up to fourth rank. This process can readily be extended to each rank-n multipole moment, yielding a hydrodynamic moment tensor with $n(n+2)$ independent components.

We have now converted the volume integrals of the stress into integrals that are completely determinate; these expressions are exact, which may be verified by application of the divergence theorem. Note that (3.15) is identical to the expression for the dipole moment obtained by Batchelor (1970) using volume averaging procedures in homogeneous suspensions, which is satisfying, and that, in in the limit of no-slip spheres with no body torques, the quadrupole moment (3.16) reduces to that obtained by Zhou & Prosperetti (2020).

The body-force and torque terms (3.15)–(3.17) can be computed in principle. This is easily done for particular flows, but it is difficult to express them in explicit form for arbitrary flows. Here, we will show that they are dynamically insignificant and can be ignored. In his study of semi-dilute suspensions, Batchelor (1977) implicitly assumed that the body force (and acceleration) terms in the dipole moment derived in Batchelor (1970) are dynamically insignificant, but the origin of the claim is opaque, because this mathematical fact does not arise naturally from the volume-averaging process. This drawback of volume averaging can be overcome using the heterogeneous-averaging methods as follows. The stress in the linear and angular momentum balances (3.3*a*) and (3.3*b*) is obtained by substituting the moments above into (2.9) to obtain the particle stress, and then utilizing (2.5) to find the suspension stress, yielding

$$-\langle p_{,i}\rangle + \eta\langle u_{i,jj}\rangle + \langle \Sigma^H_{ij,j}\rangle + \partial_j n\langle F^{(b,1)}_{ij}\rangle - \tfrac{1}{2}\partial_j\partial_k n\langle F^{(b,2)}_{ijk}\rangle + \tfrac{1}{6}\partial_j\partial_k\partial_\ell n\langle F^{(b,3)}_{ijk\ell}\rangle + \langle f_i\rangle = 0,$$
$$\varepsilon_{ijk}\langle \Sigma^H_{kj}\rangle + n\varepsilon_{ijk}\langle F^{(b,1)}_{kj}\rangle + \partial_j n\langle L^{(1)}_{ij}\rangle - \tfrac{1}{2}\partial_j\partial_k n\langle L^{(2)}_{ijk}\rangle + \langle l_i\rangle = 0,$$

where Σ^H_{ij} is the particle stress arising from the hydrodynamic multipole moments and all indeterminate terms have been included in the pressure. These expressions simplify greatly by recognizing that the body-force and torque terms appear as moment expansions of $\langle f_i\rangle$ and $\langle l_i\rangle$. The average body force and torque can be expressed using the methods of § 2, yielding the moment expansions,

$$\langle f_i\rangle = n\langle F^{(0,b)}_i\rangle - \partial_j n\langle F^{(1,b)}_{ij}\rangle + \tfrac{1}{2}\partial_j\partial_k n\langle F^{(2,b)}_{ijk}\rangle - \tfrac{1}{6}\partial_j\partial_k\partial_\ell n\langle F^{(3,b)}_{ijk\ell}\rangle + \cdots,$$
$$\langle l_i\rangle = n\langle L^{(0)}_i\rangle - \partial_j n\langle L^{(1)}_{ij}\rangle + \tfrac{1}{2}\partial_j\partial_k n\langle L^{(2)}_{ijk}\rangle + \cdots,$$

which reveals much simpler conservation laws where the high-order body force and torque moments play no dynamic role,

$$-\langle p_{,i}\rangle + \eta\langle u_{i,jj}\rangle + \langle \Sigma^H_{ij,j}\rangle + n\langle F^{(b,0)}_i\rangle = 0, \tag{3.18a}$$
$$\varepsilon_{ijk}\langle \Sigma^H_{kj}\rangle + n\varepsilon_{ijk}\langle F^{(b,1)}_{kj}\rangle + n\langle L^{(0)}_i\rangle = 0. \tag{3.18b}$$

Linear momentum conservation statements similar to (3.18*a*) have been obtained for spherical particles by Zhang & Prosperetti (1997), Jackson (1997), and angular momentum balances similar to (3.18*b*) were derived by Jackson (1997). Note that (3.18*b*) implies that the heterogeneous stress is symmetric in the absence of external (body or moment) torques, in contrast with prior works (Prosperetti 2004; Prosperetti *et al.* 2006), which predict an antisymmetric stress, and in agreement with a recent computation of the stress in suspensions of no-slip spheres (Zhou & Prosperetti 2020).

https://doi.org/10.1017/jfm.2020.6 Published online by Cambridge University Press

Here, our more general approach demonstrates that these momentum balances hold for all non-inertial heterogeneous flows.

The theoretical framework presented thus far for the stress in concentrated heterogeneous suspensions is valid for particles of arbitrary shape, size and composition, as well as arbitrary sources of heterogeneity, including non-uniform shear fields, heterogeneous force fields or spatially varying volume fractions, for instance. In the next section, we apply the theory to a specific test case, a dilute suspension of spheres, in order to ensure that the theoretical framework predicts the correct physical behaviour.

4. Constitutive equations for dilute suspensions of spheres

The overall goal of this work is the development of a method to derive a general expression for the pointwise-average stress in suspensions undergoing heterogeneous flow in terms of meso- and macroscopic quantities that can be experimentally determined. A general framework that gives a pointwise-average stress, valid for dispersions of arbitrary concentration, particle shape and particle material composition, that preserves information about the underlying microscopic dynamics was derived in §§ 2 and 3. We now seek to validate the framework for a dilute suspension by demonstrating that it produces a constitutive expression for the stress consistent with experimental observations in three distinct heterogeneous flows.

To begin, we seek to replace the number density $n(\boldsymbol{x})$ appearing in (2.9), a probabilistic, microscopic description of the particle distribution prone to temporal fluctuation, with a macroscopic, ensemble-averaged description of the particle distribution. The simplest of such distributions is the spatially varying volume fraction defined by Zhang & Prosperetti (1994*a*),

$$\phi(\boldsymbol{x}) = \langle 1 - \chi \rangle(\boldsymbol{x}), \tag{4.1}$$

which is simply the probability that a material point is located inside a particle. In homogeneous dispersions, this quantity is spatially constant and recovers the standard definition of volume fraction, $\phi = n/V_p$. More generally, for spherical particles of radius a, the volume fraction may be related to the number density by integrating the number density over the spatial extent of a particle (Zhang & Prosperetti 1994*a*)

$$\phi(\boldsymbol{x}) = \int_{|\boldsymbol{x}-\boldsymbol{y}|\leqslant a} n(\boldsymbol{y})\,\mathrm{d}\boldsymbol{y}. \tag{4.2}$$

Similar expressions for non-spherical particles may be easily obtained using the shape function $\mathcal{V}_p$ introduced in § 2. This equation can be solved for the number density, using e.g. symbolic-operator (Brenner & Haber 1984; Haber & Brenner 1984) or Fourier-transform methods, yielding an expression relating the microscopic quantity n to the macroscopic observable ϕ,

$$n(\boldsymbol{x}) = \frac{a\sqrt{\nabla^2}}{4\pi a^3 i_1(a\sqrt{\nabla^2})}\phi(\boldsymbol{x}) = \frac{3}{4\pi a^3}\left(1 - \frac{a^2}{10}\nabla^2 + \frac{9a^4}{1400}\nabla^4 + \cdots\right)\phi(\boldsymbol{x}). \tag{4.3}$$

Here, $i_1(z)$ is a modified spherical Bessel function of the first kind and $\sqrt{\nabla^2}$ is a fractional differential operator.

A similar connection to observable quantities is also required for the multipole moments appearing in (2.9). Such a relation can be obtained by returning to the

https://doi.org/10.1017/jfm.2020.6 Published online by Cambridge University Press

concept of energy dissipation. As discussed in § 3.2, the rate of work (and hence the energy dissipation rate) in a heterogeneous dispersion takes the form $\dot{W} = \mathcal{U}^{\intercal}\mathcal{F}$, where $\mathcal{U} = \{\langle u_i\rangle - U_i, \langle \gamma_{ij}\rangle, \langle e_{ij,k}\rangle, \langle e_{ij,k\ell}\rangle, \ldots\}$ is a generalized velocity vector and $\mathcal{F} = \{F_i^H, D_{ij}^H, Q_{ijk}^H, O_{ijk\ell}^H, \ldots\}$ is a generalized force vector. The energy dissipation rate, combined with the linearity of Stokes flow, implies the existence of a symmetric, grand resistance matrix $\mathcal{R}$ relating fluid and particle moments to the induced moments on the particle surface: $\mathcal{F} = \mathcal{R}\mathcal{U}$. This grand resistance matrix, along with its index and transpose symmetries, may be expressed as,

$$\begin{pmatrix} F_i^H \\ D_{ij}^H \\ Q_{ijk}^H \\ O_{ijk\ell}^H \end{pmatrix} = \begin{pmatrix} R^{FU}_{(im)} & R^{DU}_{mpi} & R^{QU}_{\{mp\}qi} & R^{OU}_{\{mp\}(qr)i} \\ R^{DU}_{ijm} & R^{D\Gamma}_{ij\,\underline{mp}} & R^{Q\Gamma}_{\{mp\}qij} & R^{O\Gamma}_{\{mp\}(qr)ij} \\ R^{QU}_{\{ij\}km} & R^{Q\Gamma}_{\{ij\}kmp} & R^{QP}_{\underline{\{ij\}k}\,\underline{\{mp\}q}} & R^{OP}_{\{mp\}(qr)\{ij\}k} \\ R^{OU}_{\{ij\}(k\ell)m} & R^{O\Gamma}_{\{ij\}(k\ell)mq} & R^{OP}_{\{ij\}(k\ell)\{mp\}q} & R^{OM}_{\underline{\{ij\}(k\ell)}\,\underline{\{mp\}(qr)}} \end{pmatrix} \begin{pmatrix} \langle u_m\rangle - U_m \\ \langle \gamma_{mp}\rangle \\ \langle e_{mp,q}\rangle \\ \langle e_{mp,qr}\rangle \end{pmatrix}, \quad (4.4)$$

where underbars represent a block symmetric tensor, i.e. $A_{\underline{i_1\ldots i_n}\,\underline{j_1\ldots j_n}} = A_{\underline{j_1\ldots j_n}\,\underline{i_1\ldots i_n}}$, and $\langle u_i\rangle$, $\langle \gamma_{ij}\rangle$, $\langle e_{ij,k}\rangle$ and $\langle e_{ij,k\ell}\rangle$ are evaluated at the particle centre. All solutions to the Stokes equations, including those from which the grand resistance matrix arises, must produce positive energy dissipation, meaning we must have the quadratic form $\mathcal{U}^{\intercal}\mathcal{R}\mathcal{U} > 0$. One way to enforce this is to require a positive definite grand resistance matrix. In the present case, the grand resistance matrix may not be positive definite, because the $\mathcal{U}$ that satisfies the pointwise-averaged Cauchy momentum equation gives a shear rate $\langle e_{ij}\rangle$ that cannot be varied independently from its gradients $\langle e_{ij,k}\rangle$ and $\langle e_{ij,k\ell}\rangle$. Indeed, these are coupled by prescription in order to smoothly connect heterogeneous flow and stress variations. However, all flows encoded into $\mathcal{U}$ are obtained from an expansion of an equation of motion that generates positive energy dissipation; hence all grand resistance matrices derived using the methods of this paper automatically produce positive dissipation. That is, any flow $\mathcal{U}$ that passes through $\mathcal{R}$ to give $\dot{W} < 0$ disobeys conservation of momentum and is not physically realizable, and thus presents no concern.

A non-positive definite grand resistance matrix is not necessarily invertible. However, any sub-blocks for which well-posed boundary value problems exist for both the force moment and velocity derivative must be positive definite and hence invertible. For instance, well-posed boundary value problems exist for both F_i^H and U_i meaning the sub-block involving $\boldsymbol{R}^{FU}$ must be positive definite. However, $\boldsymbol{R}^{QP}$ may not necessarily be invertible because there exists no well-posed physical boundary condition for Q_{ijk}^H.

Provided the resistance tensors are known, we can now express the multipole moments in terms of the observables $\langle u_i\rangle - \langle U_i\rangle$, $\langle \gamma_{ij}\rangle$, $\langle e_{ij,k}\rangle$ and $\langle e_{ij,k\ell}\rangle$. Note that the relative particle velocity $\langle u_i\rangle - \langle U_i\rangle$ can be difficult to measure in principle, and it will often prove convenient to remove it by supplementing the grand resistance matrix with a force balance on the particle. The resistance tensors for spherical particles of arbitrary composition can be obtained from solutions of six linearly independent microhydrodynamics problems, as demonstrated in appendix D. The resulting hydrodynamic resistance tensors are,

$$R^{FU}_{(ij)} = \frac{4\pi a}{3} f_1 \delta_{ij}, \quad (4.5a)$$

$$R^{D\Gamma}_{\underline{ij}\,\underline{k\ell}} = \frac{8\pi\eta a^3}{3}(s_1 \Delta^{(2,2)}_{ijk\ell} + \ell_1 \mathscr{E}^{o(2,2)}_{ijk\ell}), \quad (4.5b)$$

https://doi.org/10.1017/jfm.2020.6 Published online by Cambridge University Press

$$R^{QU}_{\{ij\}k\ell} = \frac{8\pi a^3}{3} f_2 \Delta^{(2,2)}_{ijk\ell}, \tag{4.5c}$$

$$R^{QP}_{\underline{\{ij\}k}\,\underline{\{\ell m\}p}} = \frac{8\pi\eta a^5}{3}\left(q_1^I \Delta^{(3,3)}_{ijk\ell mp} + 4q_1^R \Delta^{(2,1,2)}_{ij\alpha\beta no} \mathscr{E}^{(3,3)}_{\alpha\beta k\gamma\zeta p} \Delta^{(2,1,2)}_{\ell m\gamma\zeta no} + \frac{3q_1^D}{5} \Delta^{(2,2)}_{ijkr} \Delta^{(2,2)}_{\ell mpr}\right), \tag{4.5d}$$

$$R^{O\Gamma}_{\{ij\}(k\ell)mp} = \frac{4\pi\eta a^5}{3}\left(s_2 \Delta^{(2,2)}_{ijmp}\delta_{k\ell} + \frac{2(5\ell_1 - 3)}{15}\Delta^{(2,1,2)}_{ijmpk\ell}\right), \tag{4.5e}$$

$$R^{DU}_{ijk} = R^{Q\Gamma}_{\{ij\}k\ell m} = R^{OU}_{\{ij\}(k\ell)m} = R^{OP}_{\{ij\}(k\ell)\{mp\}q} = 0, \tag{4.5f}$$

where f_1, f_2, ℓ_1, s_1, s_2, q_1^D, q_1^R and q_1^I are flow-independent scalar coefficients that depend only on material composition. In the case of a hard sphere, $f_1 = 9/2$, $s_1 = 5/2$ and $\ell_1 = 3/2$, giving the familiar Stokes drag law (Stokes 1851), the Einstein correction to the viscosity (Einstein 1906, 1911) and the Kirchhoff law for the torque (Kirchhoff 1876), but in the form shown, (4.5) describes a sphere of any (hard, slippery, porous, viscous, etc.) material composition. Note that $\boldsymbol{R}^{OM}$ and higher-order moments need not be computed because their contributions to the stress are of $O(\eta a^4 \phi \boldsymbol{e}_{ij,kk\ell\ell})$, which are negligibly small at $O(a^4/L^4)$ provided the velocity evolves on some length scale L greater than the particle radius. The velocity of particles relative to the fluid can be obtained by rearranging the force balance,

$$m\frac{\mathrm{d}U_i}{\mathrm{d}t} = F_i^H + F_i^{(b,0)} + F_i' = \frac{4\pi a f_1}{3}(\langle u_i\rangle - U_i) + \frac{4\pi a^3 f_2}{3}\langle u_{i,jj}\rangle + F_i^{(b,0)} + F_i', \tag{4.6}$$

where F_i', the fluctuating force arising from Brownian motion and mean-field interactions with the other particles, has zero mean. The inertial term may be computed by re-expressing the total derivative as partial derivatives,

$$m\left\langle \frac{\mathrm{d}U_i}{\mathrm{d}t}\right\rangle = m\frac{\partial}{\partial t}\langle U_i\rangle + m\frac{\partial}{\partial x_j}\langle U_i U_j\rangle. \tag{4.7}$$

The first term on the right-hand side is negligible when the Stokes number is small. The second term corresponds to velocity fluctuations arising from Brownian motion, and is found to have the value $kT\partial_i \ln n$ from the Fokker–Planck equation (cf. Wilemski 1976), where k is Boltzmann's constant and T is the temperature.

We now have enough information to compute a constitutive equation for the suspension flow valid in the low Stokes and particle Reynolds number regime. The procedure is as follows: first, resistance tensors in (4.5), which are fully defined once particle boundary conditions are set, are used to compute the multipole moments D_{ij}^H, Q_{ijk}^H and $O_{ijk\ell}^H$, whereupon the force balance (4.6) is employed to eliminate terms linear in $\langle u_i\rangle - U_i$. The resultant expressions are then substituted into (2.9), the pointwise-averaged particle stress. At this point, the number density is expressed in terms of the volume fraction using (4.3), which must be truncated to the same order as the octupole moment $O_{ijk\ell}^H$, resulting in the following constitutive equation:

$$\begin{aligned}\sigma_{ij} \;=\; & -p\delta_{ij} + 2\eta^{eff}\boldsymbol{e}_{ij} - 2\mu\boldsymbol{e}_{ij,kk} - 2\eta_v\varepsilon_{ijk}(\omega_k - \Omega_k) - 2\mu_s\varepsilon_{ijk}\omega_{k,\ell\ell} \\ & + 2\alpha_I\phi_{,k}u_{\{i,jk\}} + \frac{2\alpha_R}{3}(\varepsilon_{ki\ell}\omega_{\{\ell,j\}} + \varepsilon_{kj\ell}\omega_{\{\ell,i\}})\phi_{,k} + \frac{3\alpha_D}{5}\phi_{,k}\Delta^{(2,2)}_{ijk\ell}u_{\ell,mm} \\ & - 2(\varepsilon_{j\ell k}\partial_i\partial_\ell + \varepsilon_{i\ell k}\partial_j\partial_\ell)\mu_s(\omega_k - \Omega_k) + 2\partial_k\zeta\,\Delta^{(2,2)}_{ijk\ell}f_\ell^{(b,0)} - \frac{2kT}{V_p}\partial_k\zeta\,\Delta^{(2,2)}_{ijk\ell}\partial_\ell\ln\phi,\end{aligned} \tag{4.8}$$

https://doi.org/10.1017/jfm.2020.6 Published online by Cambridge University Press

where ensemble averages have been dropped for ease of readability, $f_i^{(0)} = F_i^{(0,b)}/V_p$ is the average body force per unit volume and we have excluded all terms of $O(\eta\phi a^4 e_{ij,kk\ell\ell})$ and higher. The transport coefficients emerge naturally as

$$\eta^{eff} = \eta\left(1 + s_1\phi - \left(\frac{a^2}{10}s_1 - \frac{a^2}{2}s_2\right)\phi_{,kk}\right), \tag{4.9a}$$

$$\mu = \eta a^2\phi\left(\frac{8}{15}q_1^I + \frac{3}{10}q_1^D + \frac{1}{6}q_1^R - \frac{f_2^2}{f_1} - s_2\right), \tag{4.9b}$$

$$\eta_v = \eta\ell_1\left(\phi - \frac{a^2}{10}\phi_{,kk}\right), \tag{4.9c}$$

$$\mu_s = \eta a^2\phi\frac{5\ell_1 - 3}{30}, \tag{4.9d}$$

$$\alpha_I = \eta a^2(s_2 - q_1^I), \tag{4.9e}$$

$$\alpha_R = \eta a^2(s_2 - q_1^R), \tag{4.9f}$$

$$\alpha_D = \eta a^2\left(\frac{10}{3}\frac{f_2^2}{f_1} + s_2 - q_1^D\right), \tag{4.9g}$$

$$\zeta = a^2\frac{f_2}{f_1}\phi. \tag{4.9h}$$

Here, η^{eff} is the effective viscosity, η_v is the vortex viscosity, μ is the shear-curvature viscosity encoding the non-local influence of the shear rate and μ_s is the spin viscosity, which gives the stress resulting from heterogeneous body torque fields. The anisotropy coefficients α_I, α_R and α_D encode the loss of isotropy associated with the development of concentration gradients in the suspension, and the transport coefficient ζ is a 'force-gradient viscosity' arising from heterogeneous body forces and the resulting gradients in particle velocity. The term involving $\ln\phi$ is a dissipative stress arising from the particle flux and resultant fluid motion induced by chemical potential gradients. This term is of no dynamic consequence as it may be included in a redefined pressure; however, it serves to illustrate that the suspension supports no deviatoric stresses at thermodynamic equilibrium, i.e. when ϕ is Boltzmann distributed.

This constitutive equation is quite different from prior constitutive equations or transport equations for colloids (Jackson 1997; Zhang & Prosperetti 1997; Prosperetti 2004) that include the particle velocity (as a kinematic variable). These prior works point out that (using our notation) $\boldsymbol{R}^{QU} \sim \eta a^3$ whereas $\boldsymbol{R}^{QP} \sim \boldsymbol{R}^{O\Gamma} \sim a^5\eta$, and thus they assert that the leading-order heterogeneous correction to the stress arises from the velocity *difference* $\langle u_i\rangle - \langle U_i\rangle$. However, conservation of momentum on a particle as given by (4.6) shows that $\boldsymbol{R}^{QU}$ enters the momentum balance at the same order as $\boldsymbol{R}^{QP}$ and $\boldsymbol{R}^{O\Gamma}$, and thus these terms cannot be neglected. Jin *et al.* (2018) have correctly included these higher-order couplings in their derivation of the value of μ for dilute suspensions of no-slip spheres. However, their results were limited to computation of μ only and, as will be shown below, errors in their analysis resulted in a value of the shear-curvature viscosity $\mu = \eta a^2\phi/10$ inconsistent with physical constraints on μ.

Thermodynamic physical constraints on μ from continuum constitutive equations suggest a positive value of μ (Eringen 1966; Stokes 1966; Bleustein & Green 1967) in contrast with experimental observations of $\mu < 0$. For instance, the functional form of the pair diffusivity measured in microrheology experiments of F-actin networks

https://doi.org/10.1017/jfm.2020.6 Published online by Cambridge University Press

(Sonn-Segev *et al.* 2014) can be shown to be consistent with negative values of μ when compared with point force velocity solutions of e.g. the micropolar fluid (Ramkissoon & Majumdar 1976). Similar theory/experiment conflicts exist in solid mechanics (Maranganti & Sharma 2007; Askes & Aifantis 2011), where continuum thermodynamic arguments again predict positive values of the elastic equivalents of μ, whereas lattice models (Chang & Gao 1995), molecular dynamics simulations (Maranganti & Sharma 2007) and experimental measurements (Jakata & Every 2008) all predict negative $\mu < 0$.

We believe that the weight of evidence suggests that $\mu < 0$, in contrast with the thermodynamic predictions of $\mu > 0$, suggesting that the computation of Jin *et al.* (2018) is incorrect. This conflict can be reconciled by recognizing that the thermodynamic constraints in the continuum models arise from an assumption that constitutive models employing μ are exact descriptions over all length scales. It is well known that $\mu > 0$ leads to thermodynamic instabilities only for very large shear-rate gradients (Askes & Aifantis 2011). However, the heterogeneous constitutive models discussed here are inherently perturbative in nature, with $\mu\nabla^2 e_{ij}$ providing the leading-order correction for non-local behaviour in the shear rate. Thus, very large gradients are outside the range of validity of the results and application of thermodynamic constraints at arbitrary length scales will lead to spurious results. A similar phenomenon has been seen in weakly nonlinear constitutive equations such as the second-order fluid models, where thermodynamic bounds on coefficients derived at high shear rates lead to negative relaxation times (Aksel 2002).

Constraints on other model parameters may be obtained by comparing our model to experiments and simulation. Stokesian dynamics simulations of colloids in a rheometer of gap width H have reported that the high-frequency viscosity of the suspensions increases with decreasing H (Swan & Brady 2011). Similar behaviours are observed in the steady shear viscosity of polydisperse suspensions, where polydispersity prevents shear-induced ordering (Ramaswamy *et al.* 2017). The influence of confinement on stress obtained from our heterogeneous-averaging method can be found by volume averaging of the effective viscosity in (4.9) over the interior of a rheometer of width H, which yields,

$$\frac{1}{V}\int \eta^{eff}\,\mathrm{d}V = \eta\left(1+\phi s_1 - \frac{a}{H}\left(\frac{a}{10}s_1 - \frac{a}{2}s_2\right)\frac{\partial\phi}{\partial n}\right),$$

where $\partial\phi/\partial n$ is the normal derivative of the volume fraction evaluated at the rheometer wall. Because the volume fraction is identically zero at the wall and increases towards the bulk, this normal derivative is always negative. Thus, replicating observed increases in viscosity with decreasing gap width requires that

$$s_1 \geqslant 5s_2. \tag{4.10}$$

As will be shown below, this is equivalent to the statement that of all dilute suspensions of spherical particles of a given material composition, solid spheres with no-slip boundary conditions maximize the energy dissipation.

Constraints on the anisotropy coefficients α_I, α_D and α_R may be found by examining the problem of pressure-driven flow in a pipe. It is well known that particles tend to move toward the centreline in pressure-driven flow of particle laden dispersions at vanishingly small Reynolds number (Koh *et al.* 1994; Lyon & Leal 1998*a*,*b*; Frank *et al.* 2003); the underlying mechanism is shear-induced migration, which is distinct

https://doi.org/10.1017/jfm.2020.6 Published online by Cambridge University Press

from the inertial Segré–Silberberg effect where particles accumulate in a region located between the wall and the centreline (Segre & Silberberg 1961). In order to be consistent with these experiments, our model must predict particle migration. At low volume fractions, it is observed that the velocity profile in the pipe remains nearly parabolic despite particle migration (Koh *et al.* 1994; Frank *et al.* 2003), whereas it exhibits significant blunting in concentrated suspensions (Lyon & Leal 1998*a*,*b*). We will, in light of these experimental observations, examine the stress tensor predicted by (4.8) for a parabolic velocity profile, and determine the values of α_I, α_R and α_D for which particle migration occurs.

The position-dependent part of pressure-driven flow through a planar or circular duct may be represented as

$$u_i(\boldsymbol{x}) = \tfrac{1}{2} P_{ijk} x_j x_k, \quad P_{ijk} = m_i(n_i n_j + \lambda q_i q_j), \tag{4.11}$$

where n_i, n_i and q_i are three mutually orthogonal vectors and λ controls the shape of the pipe; $\lambda = 0$ corresponds to planar Poiseuille flow and $\lambda = 1$ corresponds to a circular duct. Substituting (4.11) into (4.8) yields

$$\sigma_{ij} = -p\delta_{ij} + 2P_{(ij)k}\left[\eta^{eff} x_k + \left(\frac{2(4-\lambda)}{15}\alpha_I + \frac{1-\lambda}{6}\alpha_R + \frac{3(1+\lambda)}{10}\alpha_D\right)\phi_{,k}\right], \tag{4.12}$$

where we have assumed that the volume-fraction gradient is directed along the velocity gradient. Bounds on the anisotropy coefficients can be found by invoking the assumption that particle migration towards the centreline reduces energy dissipation and the stress. The gradient $\phi_{,i}$ is oriented opposite to x_i when particles move to the centreline. Thus, the quantity in parentheses in (4.12) must be positive to reduce dissipation. Two inequalities may be obtained by separately considering the cases $\lambda = 0$ and $\lambda = 1$,

$$\frac{8\alpha_I}{15} + \frac{\alpha_R}{6} + \frac{3\alpha_D}{10} \geqslant 0, \quad 2\alpha_I + 3\alpha_D \geqslant 0. \tag{4.13}$$

The first inequality gives $\mu \leqslant 0$ which, as discussed above, is consistent with experimental observations. The fact that two distinct experimental observations produce restrictions that are also consistent with thermodynamics is satisfying and encouraging.

Constraints can be placed on the vortex viscosity η_v and the force-gradient viscosity ζ by recognizing that they have a close dynamic relationship with the shear viscosity, in that they each couple gradients of a field to the stress. This similarity suggests that both the vortex and force-gradient viscosities are positive numbers for spatially uniform volume fraction, which requires,

$$\ell_1 \geqslant 0, \tag{4.14}$$

$$\zeta \geqslant 0. \tag{4.15}$$

It is well established from energy dissipation methods that the vortex viscosity must be positive (Grad 1952). We are unaware of corresponding results in the literature for the force-gradient viscosity.

We now show that our averaging method produces physically valid results by computing explicit values of the constitutive parameters for particular boundary

https://doi.org/10.1017/jfm.2020.6 Published online by Cambridge University Press

conditions on the sphere surfaces. Many physical systems of interest have no-penetration boundary conditions $n_i u_i = 0$, meaning the sphere maintains a spherical shape and there is no mass flux across the interface. This restriction leads to a set of relationships between coefficients (cf. appendix D),

$$f_2 = \frac{f_1 - 3}{2}, \quad s_2 = \frac{s_1 - 1}{3}, \quad q_1^D = \frac{5f_1}{6} - 3. \tag{4.16a–c}$$

Thermodynamic arguments may be invoked to derive further bounds on the coefficients. If the surface of the sphere is not active, we expect the rate of energy dissipated by surface forces to be positive, requiring $\int u_i \sigma_{ij} n_j \, \mathrm{d}S \geqslant 0$, which implies

$$3 \leqslant f_1 \leqslant \tfrac{9}{2}, \quad 1 \leqslant s_1 \leqslant \tfrac{5}{2}, \quad 0 \leqslant \ell_1 \leqslant \tfrac{3}{2}, \quad \tfrac{1}{8} \leqslant q_1^I \leqslant \tfrac{7}{16}, \quad -\tfrac{1}{4} \leqslant q_1^R \leqslant 1. \tag{4.17a–e}$$

As shown below, these resistance scalars are bounded from below by the results of completely slip spheres, and from above by rigid, no-slip spheres. These sets of restrictions imply that the constraints (4.10), (4.14) and (4.15) are automatically satisfied by all impermeable spheres.

The efficacy of the framework presented in this work can be tested by computing the material coefficients in (4.9) for specific materials. We will examine two physical systems. The first case we consider is spherical droplets of viscosity $\lambda\eta$, with boundary conditions of no slip, impermeability and continuity of the tangential traction on the particle surface,

$$u_i^p = u_i^f, \quad n_i u_i^f = 0, \quad \lambda\eta(\delta_{ij} - n_i n_j) e_{jk}^p n_k + \tfrac{1}{2}\varepsilon_{ijk} l_k n_j = \eta(\delta_{ij} - n_i n_j) e_{jk}^f n_k. \tag{4.18a–c}$$

Here, we have explicitly included an antisymmetric stress interior to the particle (i.e. the body torque) in the tangential momentum balance. Neglecting this term, as was done in prior works (Hetsroni & Haber 1970), would lead to the erroneous conclusion that $\ell_1 = 0$ for droplets. The case $\ell_1 = 0$ would in turn imply that a droplet cannot support a hydrodynamic torque, which is at odds with the fact that an infinite viscosity droplet, i.e. a no-slip sphere, does support a torque (Kirchhoff 1876). These boundary conditions yield the coefficients (cf. appendix D)

$$f_1 = \frac{3}{2}\frac{3\lambda + 2}{\lambda + 1}, \quad \ell_1 = \frac{3}{2}, \quad s_1 = \frac{1}{2}\frac{5\lambda + 2}{\lambda + 1}, \quad q_1^I = \frac{1}{16}\frac{7\lambda + 2}{\lambda + 1}, \quad q_1^R = \frac{\lambda - 1}{\lambda + 4}. \tag{4.19a–e}$$

Secondly, we consider spheres with the Navier-slip condition

$$u_i^f = \frac{a}{\eta\beta}(\delta_{ij} - n_i n_j)\sigma_{jk}^f n_k, \tag{4.20}$$

where the dimensionless slip parameter β controls the degree of slip; $\beta \to 0$ corresponds to perfect slip while $\beta \to \infty$ recovers the no-slip limit. This boundary condition yields the coefficients (cf. appendix D)

$$f_1 = \frac{9}{2}\frac{\beta + 2}{\beta + 3}, \quad \ell_1 = \frac{3}{2}\frac{\beta}{\beta + 3}, \quad s_1 = \frac{5}{2}\frac{\beta + 2}{\beta + 5}, \quad q_1^I = \frac{7}{16}\frac{\beta + 2}{\beta + 7}, \quad q_1^R = \frac{\beta - 1}{\beta + 4}. \tag{4.21a–e}$$

https://doi.org/10.1017/jfm.2020.6 Published online by Cambridge University Press

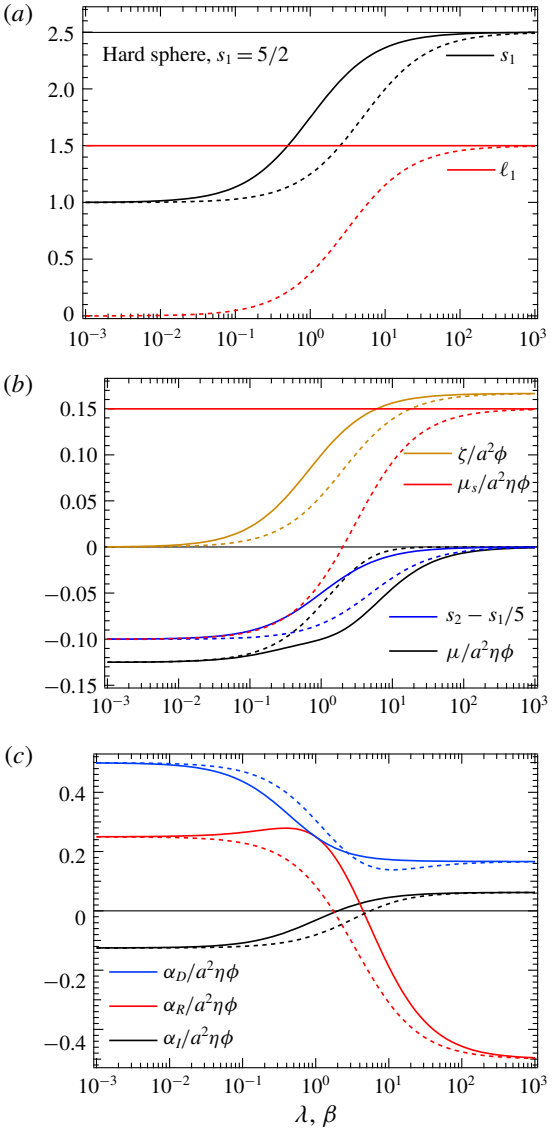


FIGURE 2. Plots of the transport coefficients defined in (4.9) that appear in the constitutive equation for heterogeneous suspensions. Solid lines indicate results for droplets of viscosity ratio λ and dotted lines indicate Navier-slip spheres with slip parameter β. (*a*) Intrinsic viscosity s_1 and intrinsic vortex viscosity ℓ_1 for droplets (solid) and Navier-slip spheres (dashed). The parameters asymptote to the same hard-sphere value. The Einstein correction $s_1 = 5/2$ is shown for reference. (*b*) The leading-order corrections for heterogeneity, the force-gradient viscosity ζ, the spin viscosity μ_s, the heterogeneous correction to the viscosity $s_2 - s_1/5$ and the shear-curvature viscosity μ for droplets (solid) and Navier-slip spheres (dashed). The shear-curvature viscosity is non-positive, as required. (*c*) The anisotropy coefficients α_D, α_R and α_I for droplets (solid) and Navier-slip spheres (dashed). The plotted values of the coefficients predict particle margination in pressure-driven flow for all λ and β.

https://doi.org/10.1017/jfm.2020.6 Published online by Cambridge University Press

We applied these coefficients to compute the values of constitutive parameters in (4.9), which are plotted in figure 2 as a function of the dimensionless droplet viscosity λ and the dimensionless slip length β. We begin our discussion with the homogeneous stress terms s_1 (the intrinsic viscosity) and ℓ_1 (the intrinsic vortex viscosity), plotted in figure 2(*a*). The values plotted for s_1 recover prior computations of the intrinsic viscosity of suspensions of droplets (Taylor 1932) and Navier-slip spheres (Felderhof 1976). The values of intrinsic viscosity for droplets and Navier-slip spheres are similar, asymptoting to values of $s_1 = 1$ for in the limits $\beta, \lambda \to 0$ and recovering the famous Einstein correction $s_1 = 5/2$ (Einstein 1906, 1911) in the limit $\beta, \lambda \to \infty$. In contrast, the vortex viscosity is qualitatively different for droplets and Navier-slip spheres. The intrinsic vortex viscosity, as given by ℓ_1 is independent of λ for droplets, whereas it is a function of β for Navier-slip spheres. This differing behaviour arises from the tangential stress balance, which demonstrates that droplets will undergo solid-body rotation in response to applied body torques, revealing a hydrodynamic torque independent of drop viscosity. In contrast, the tangential stress for the Navier-slip spheres decreases as the fluid slips across the surface with increasing slip length, eventually vanishing in the infinite slip limit ($\beta \to 0$).

New results arising from the present heterogeneous model are shown in figure 2(*b*,*c*). The relationship between these parameters and experimental observations was discussed above, and here we plot their numerical values to ensure that our model agrees with experiments. The shear-curvature viscosity μ, the force-gradient viscosity ζ, the spin viscosity μ_s and the heterogeneous correction to η^{eff} are plotted in figure 2(*b*). Equations (4.9) and (4.16) indicate that the vortex viscosity and the heterogeneous correction to the viscosity are completely specified by s_1 and ℓ_1, and thus exhibit identical behaviours to those in figure 2(*a*). The force-gradient viscosity ζ is seen to be positive for all finite values of β and λ, as required by (4.15). We find that $\zeta \to 0$ in the limits of full slip or inviscid droplets, i.e. $\beta, \lambda \to 0$. Physically, this is because an inviscid droplet produces no tangential surface traction when acted on by a body force (cf. appendix D), and hence can only modify the average suspension pressure $\langle p \rangle$.

The shear-curvature viscosity μ asymptotes to zero for the hard-sphere limit, i.e. $\lambda, \beta \to \infty$, and is strictly negative for all other values, as required from experimental observations discussed above (Maranganti & Sharma 2007; Jakata & Every 2008). The value $\mu = 0$ for hard spheres computed using our heterogeneous-averaging techniques corrects prior literature values obtained using different methods. The value of $\mu = \eta a^2 \phi/10$ calculated by Jin *et al.* (2018) using the heterogeneous-averaging method of Dhont & Briels (2002) arises from an algebraic error in the computation of S^H_{ij} (in our notation); this error can be observed in their expression for S^H_{ij} (their equation (11)), which is inconsistent with the well-known Faxén laws for the stresslet of no-slip spheres (Batchelor & Green 1972*a*). Raja *et al.* (2010) obtained a value of $\mu = -\eta a^2 \phi/10$ using a method that neglected the heterogeneous stress moments, i.e. Q^H_{ijk} and $O^H_{ijk\ell}$.

To complete our discussion of the results, we plot α_I, α_R and α_D in figure 2(*c*). It is observed that the second inequality in (4.13) is satisfied for all values of β and λ, while the first constraint has already been satisfied by the observed $\mu \leqslant 0$ in figure 2(*b*). This confirms that the values of α_I, α_R and α_D predicted from our models are consistent with experimental observations of particle margination in pressure-driven flows (Koh *et al.* 1994; Lyon & Leal 1998*a*,*b*; Frank *et al.* 2003). With this constraint satisfied, we find that our model is consistent with all experimental studies examined, demonstrating the utility of utilizing the mathematical framework presented in §§ 2 and 3 to derive constitutive equations for heterogeneously deformed dispersions.

https://doi.org/10.1017/jfm.2020.6 Published online by Cambridge University Press

5. Conclusions

We have presented a theoretical framework for the derivation of non-local constitutive equations in colloidal dispersions of arbitrary concentration and composition. We employed heterogeneous ensemble-averaging techniques to obtain the statistically averaged stress at a material point in a dispersion of particles of arbitrary shape and material composition at arbitrary concentration. A series expansion of the heterogeneous averages revealed that the stress contains multipole moments that encode spatial correlations between the statistical properties of the suspension at nearby material points. An angular momentum balance was used to show that the multipole moments, and hence the average stress tensor, are symmetric in the absence of externally applied torques, resolving a long standing impediment present in prior work (Prosperetti 2004; Prosperetti *et al.* 2006). Tensorial symmetries encoding the physical behaviours of the suspension were extracted through a harmonic decomposition of the multipole moments, revealing the presence of dynamically insignificant terms that may be discarded without loss of generality. The decomposed moments were converted into surface integrals of the hydrodynamic traction and fluid velocity using energy methods to facilitate their evaluation. Overall, the advancement of this work was the development of a mathematical framework that can be used to predict the material properties of heterogeneous dispersions.

We utilized this framework to derive constitutive equations for dilute suspensions of spherical particles in heterogeneous flows, showing that the stress contains non-local corrections for statistical heterogeneities in fluid velocity, particle volume fraction and externally applied force and torques. Explicit values of the constitutive parameters in the model were obtained for spherical droplets and rigid spheres with Navier-slip boundary conditions. Application of the model to two model problems, confined shear rheology and pressure-driven flow, showed that the values obtained for the constitutive parameters are consistent with experimentally observed phenomena. We further provided a potential resolution of the sign paradox associated with several non-local continuum models, arguing that this apparent paradox arises from applying a perturbative model outside its range of validity.

Extension to non-dilute suspensions can be obtained by coupling the methods presented here with a Smoluchowski equation for a heterogeneous pair distribution function. The long-ranged nature of hydrodynamic interactions between particle pairs may introduce long-ranged non-local couplings in concentrated suspensions that need to be renormalized. We believe it is possible to renormalize such divergent integrals by utilizing phase-averaging techniques to ensemble average the integral representation of Stokes flow (Ladyzhenskaya 1969) over the domain bounded by the particle surfaces and a fictitious far-field surface. The integral representation evaluated at this far-field surface, by its very nature, will account for backflow induced by particles outside the domain of consideration, cancelling divergent interactions between particles and providing a generalization of existing volume-averaged renormalization techniques (O'Brien 1979). Furthermore, one could imagine employing our mathematical framework in conjunction equations of motion for deformable particles (Gao, Hu & Castañeda 2011; Zakhari, Anderson & Hütter 2018) to compute constitutive equations for suspensions in which the particles themselves are undergoing heterogeneous deformations. In the future, it may be possible to utilize, e.g. symbolic operator methods (Brenner & Haber 1984; Haber & Brenner 1984), to compute an arbitrary number of terms in the multipole expansions, potentially allowing for direct computation of a heterogeneous stress kernel in both dilute and non-dilute suspensions of particles of arbitrary shape.

https://doi.org/10.1017/jfm.2020.6 Published online by Cambridge University Press

Acknowledgements

The authors thank an anonymous reviewer for insightful comments that lead to a simplification in the derivations of our main results. This work was supported in part by an Office of Naval Research Young Investigator Award (no. N00014-14-1-0744).

Declaration of interests

The authors report no conflict of interest.

Appendix A. Rate of energy dissipated by surface forces

The total rate of work done by surface forces in a dispersion may be expressed as

$$\dot{W} = \int_{S_\infty} u_i^f \sigma_{ij}^f \tilde{n}_j \,\mathrm{d}S, \tag{A 1}$$

where S_∞ is the bounding surface of suspension, or, if the suspension is infinite, a fictitious surface far from the particles, and $\tilde{n}_i$ is the unit normal pointing out of the domain. We extract the portion of the work that does not vanish when the particles are replaced with fluid following the approach of § 2, yielding

$$\int_{S_\infty} (\langle u_i \rangle - U_i - \varepsilon_{i\ell m}\Omega_\ell r_m)(\langle \sigma_{ij} \rangle - \langle \Sigma_{ij} \rangle)\tilde{n}_i \,\mathrm{d}S, \tag{A 2}$$

where we have adopted a reference frame moving with the particle. Subtracting (A 2) from (A 1) yields

$$\begin{aligned}\int_{S_\infty} (\langle u_i \rangle - U_i - \varepsilon_{i\ell m}\Omega_\ell r_m)\sigma_{ij}^f \tilde{n}_j \,\mathrm{d}S - \int_{S_\infty} u_i^f (\langle \sigma_{ij} \rangle - \langle \Sigma_{ij} \rangle)\tilde{n}_i \,\mathrm{d}S \\ - \int_{S_\infty} (\langle u_i \rangle - U_i - \varepsilon_{i\ell m}\Omega_\ell r_m - u_i^f)(\sigma_{ij}^f + \langle \sigma_{ij} \rangle - \langle \Sigma_{ij} \rangle)\tilde{n}_j \,\mathrm{d}S.\end{aligned} \tag{A 3}$$

The integral on the second line vanishes under the closure relation given by (3.2). Note that this closure relation may not be used to simplify integrals involving the stress, as the stress tends to $\langle \sigma_{ij} \rangle$ rather than $\langle \sigma_{ij} \rangle - \langle \Sigma_{ij} \rangle$ under the closure relation. Application of the divergence theorem to (A 3) yields (3.7) in the main text,

$$\int_{S_p} (\langle u_i \rangle - U_i - \varepsilon_{i\ell m}\Omega_\ell r_m)\sigma_{ij} n_j \,\mathrm{d}S - \int_{S_p} (\langle \sigma_{ij} \rangle - \langle \Sigma_{ij} \rangle) n_j u_i^f \,\mathrm{d}S.$$

Appendix B. Harmonic decomposition of a third-rank tensor

Harmonic decomposition is a method where by a tensor is decomposed into irreducible tensors. From the Clebsch–Gordan theorem (Auffray 2013), a general third-rank tensor decomposes into a septor (rank-3 tensors), two pseudo-deviators (rank-2), three vectors and a pseudo-scalar. This decomposition is non-unique due to the multiplicities of deviators and vectors. For our purposes, it is convenient to employ the orthogonal decomposition given by (Zou *et al.* 2001),

$$A_{ijk} = S_{ijk} + \Delta^{(2,2)}_{ij\ell m}\varepsilon_{\ell pk} D^{(1)}_{mp} + \varepsilon_{ij\ell} D^{(2)}_{\ell k} + \Delta^{(2,2)}_{ijk\ell} v^{(1)}_\ell + \mathscr{O}^{(2,2)}_{ijk\ell} v^{(2)}_\ell + \delta_{ij} v^{(3)}_k + \varepsilon_{ijk} s. \tag{B 1}$$

Explicit expressions for the tensors in this expression can be found by contracting the left-hand side of (B 1) with isotropic tensors. For instance, contraction with the

https://doi.org/10.1017/jfm.2020.6 Published online by Cambridge University Press

alternating symbol yields $s = \varepsilon_{ijk}A_{ijk}/6$. This process can be repeated for each tensor, and may be summarized in operator form as

$$\begin{aligned} I^{(3,3)}_{ijk\ell mp} &= \Delta^{(3,3)}_{ijk\ell mp} + 4\Delta^{(2,1,2)}_{ij\alpha\beta no}\mathscr{E}^{(3,3)}_{\alpha\beta k\gamma\zeta p}\Delta^{(2,1,2)}_{\ell m\gamma\zeta no} + 3\mathscr{E}^{(3,3)}_{ijq\ell mr}\Delta^{(2,2)}_{kqpr} \\ &\quad + \tfrac{3}{5}\Delta^{(2,2)}_{ijkr}\Delta^{(2,2)}_{\ell mpr} + \mathscr{E}^{(2,2)}_{ijkr}\mathscr{E}^{(2,2)}_{\ell mpr} + \tfrac{1}{3}\delta_{ij}\delta_{kp}\delta_{\ell m} + \mathscr{E}^{(3,3)}_{ijk\ell mp}, \end{aligned} \tag{B 2}$$

where $I^{(3,3)}$ projects a third-rank tensor onto itself and each tensor in (B 2) extracts an irreducible component tensor of A_{ijk}. The isotropic tensor operators appearing in these expressions are defined as,

$$\Delta^{(2,2)}_{ijk\ell} = \tfrac{1}{2}(\delta_{ik}\delta_{j\ell} + \delta_{i\ell}\delta_{jk}) - \tfrac{1}{3}\delta_{ij}\delta_{k\ell}, \tag{B 3a}$$

$$\begin{aligned} \Delta^{(3,3)}_{ijk\ell mp} &= \tfrac{1}{3}(\delta_{i\ell}\Delta^{(2,2)}_{jkmp} + \delta_{im}\Delta^{(2,2)}_{jk\ell p} + \delta_{ip}\Delta^{(2,2)}_{jk\ell m}) \\ &\quad - \tfrac{2}{15}(\delta_{\ell m}\Delta^{(2,2)}_{ipjk} + \delta_{\ell p}\Delta^{(2,2)}_{imjk}\delta_{mp}\Delta^{(2,2)}_{i\ell jk}), \end{aligned} \tag{B 3b}$$

$$\mathscr{E}^{(2,2)}_{ijk\ell} = \tfrac{1}{2}\varepsilon_{ijm}\varepsilon_{k\ell m}, \tag{B 3c}$$

$$\mathscr{E}^{(3,3)}_{ijk\ell mp} = \tfrac{1}{6}\varepsilon_{ijk}\varepsilon_{\ell mp}, \tag{B 3d}$$

$$\Delta^{(2,1,2)}_{ijk\ell mp} = \Delta^{(2,2)}_{ijq\alpha}\mathscr{E}^{(2,2)}_{q\beta k\ell}\Delta^{(2,2)}_{\alpha\beta mp}. \tag{B 3e}$$

and are described in § 3.2.

Appendix C. Harmonic decomposition of the octupole moment

Computation of the octupole moment requires more careful analysis than the quadrupole. We begin with the operator

$$\tfrac{1}{2}\Delta^{(2,2)}_{ijmp}(\delta_{kq}\delta_{\ell r} + \delta_{kr}\delta_{\ell q}),$$

which projects a A_{mpqr} into a tensor that is irreducible in the first two indices, and symmetric in the second two, i.e. the symmetries of the hydrodynamic octupole moment. However, this operator does not encode all symmetries of the octupole moment, as due to incompressibility, any term in the octupole that enters the momentum balance as the gradient of a scalar is indeterminate. We seek to remove such indeterminate terms from the operator using harmonic decomposition.

The octupole is irreducible in the first index pair and symmetric in the second pair. From the Clebsch–Gordan rule (Auffray 2013), the octupole moment must then decompose into one fourth-rank nonor, one pseudo-septor, two deviators, one pseudo-vector and one scalar. These tensors may then be projected back into the space of rank-four tensors as

$$\begin{aligned} O^{H}_{ijk\ell} &= O^{(4)}_{ijk\ell} + \Delta^{(2,2)}_{ijmp}\varepsilon_{mkq}O^{(3)}_{qp\ell} + \Delta^{(2,2)}_{ijmp}\varepsilon_{m\ell q}O^{(3)}_{qpk} + (\Delta^{(3,3)}_{ij(k\ell)mp} - \tfrac{8}{15}\Delta^{(2,2)}_{ijmp}\delta_{k\ell})\left(O^{(2,1)}_{mp} + O^{(2,2)}_{mp}\right) \\ &\quad + \Delta^{(3,3)}_{ij(k\ell)mp}O^{(2,1)}_{mp} + 2\Delta^{(2,1,2)}_{ijmpk\ell}\varepsilon_{mpq}O^{(1)}_{p} + \Delta^{(2,2)}_{ijk\ell}O^{(0)}. \end{aligned}$$

Contraction of the octupole moment with $\partial_j\partial_k\partial_\ell$ reveals that the scalar term $O^{(0)}$ and the term involving the sum $O^{(2,1)}_{mp} + O^{(2,2)}_{mp}$ are indeterminate and can be removed without loss of generality. In Stokes flow, harmonicity of the rotation rate, i.e. $\omega_{i,jj} = 0$, also leads to the conclusion that the pseudo-vector $O^{(1)}_i$ is dynamically indeterminate

https://doi.org/10.1017/jfm.2020.6 Published online by Cambridge University Press

(Brunn 1980); however, this dynamic indeterminacy does not extend to heterogeneous suspensions, and $O_i^{(1)}$ cannot be removed. As a consequence, the far-field stress equation (3.12), which assumes a Stokesian pressure field, fails to give a correct expression for $Q_i^{(1)}$. This requires the addition of a correction, involving a volume integral of the velocity, to ensure the correct form of the volume integrals are obtained upon application of the divergence theorem.

However, this correction provides no difficulty in evaluation of the octupole moment. The fact that there are only three dynamically significant octupole moments in Stokes flow implies that $O_i^{(1)}$ must depend linearly on the other moments. For instance, it is shown in appendix D that $O_i^{(1)}$ can be determined for rotating spheres by combining generalized Faxén relations with the symmetry of the grand resistance matrix. The dynamically indeterminate terms in the octupole moment are then found by solving for $O^{(0)}$, $O_{ij}^{(2,1)}$ and $O_{ij}^{(2,2)}$ through various index contractions,

$$O^{(0)} = \tfrac{1}{5}\Delta^{(2,2)}_{ijk\ell} O^H_{ijk\ell}, \tag{C 1}$$

$$O^{(2,1)}_{ij} = \tfrac{75}{56}\Delta^{(3,3)}_{ij(k\ell)mp} O^H_{k\ell mp}, \tag{C 2}$$

$$O^{(2,2)}_{ij} = \tfrac{75}{8}(\Delta^{(3,3)}_{ij(k\ell)mp} - \tfrac{8}{15}\Delta^{(2,2)}_{ijmp}\delta_{k\ell}) O^H_{k\ell mp}. \tag{C 3}$$

The final form of the octupole moment is then obtained by removing the dynamically insignificant terms from the octupole, and then adding the required correction term to $O_i^{(1)}$. The resulting expression will contain one nonor (nine components), one pseudo-septor (seven components), one deviator (five components) and one pseudo-vector (three components), for a total of 24 components.

Appendix D. Stokes flow singularities

Here, we will compute the velocity disturbance and stress moments induced on a sphere by the ambient flow. The far-field boundary condition for the flow is given by (3.2), which states that the velocity tends towards its average value. We employ the Taylor expansion of this far-field velocity given in (3.10), which is decomposed harmonically using (B 2), yielding

$$\begin{aligned} u_i \;\to\; & \langle u_i\rangle + \varepsilon_{ijk}\langle\omega_j\rangle r_k + \langle e_{ij}\rangle r_j + \tfrac{1}{2}\langle u_{i,jk}\rangle r_j r_k \\ & - \tfrac{2}{3}\varepsilon_{ij\ell} r_j \langle\omega_{k,\ell}\rangle r_k + \tfrac{1}{10}(2r^2\delta_{ij} - r_i r_j)\langle u_{j,kk}\rangle \quad \text{as } r\to\infty, \end{aligned} \tag{D 1}$$

where we have, without loss of generality, set $U_i = \Omega_i = 0$. A similar approach was employed by Nadim & Stone (1991) in computing the deformation of a sphere in a quadratic flow. The chief advantage of this formulation is that the far-field boundary condition now represents orthogonal, linearly independent flows.

The disturbance velocity propagated by a sphere must be linear in the far-field velocity, and can be expressed using singularity methods as

$$\begin{aligned} \frac{3(u_i - \langle u_i\rangle)}{4\pi\eta a} \;=\; & -(f_1 + a^2 f_2\nabla^2) J_{ij}\langle u_j\rangle + 2a^2\left(\left(s_1 + \frac{a^2 s_2}{2}\nabla^2\right)\langle e_{jk}\rangle - \ell_1\varepsilon_{jk\ell}\langle\omega_\ell\rangle\right) J_{ij,k} \\ & - 2a^4\left((q_1^I + a^2 q_2^I\nabla^2)\langle u_{\{j,k\ell\}}\rangle - \frac{2q_1^R}{3}\varepsilon_{jkm}\langle\omega_{\{m,\ell\}}\rangle + \frac{3q_1^D}{20}\delta_{k\ell}\langle u_{j,mm}\rangle\right) J_{ij,k\ell} \\ & - a^2 f_2 J_{ij}\langle u_{j,kk}\rangle, \end{aligned} \tag{D 2}$$

https://doi.org/10.1017/jfm.2020.6 Published online by Cambridge University Press

where

$$J_{ij} = \frac{1}{8\pi\eta}\left(\frac{\delta_{ij}}{r} + \frac{r_i r_j}{r^3}\right)$$

is the fundamental solution of the Stokes equations, i.e. the Stokeslet. The appearance of f_2 in the $\langle u_{i,jj}\rangle$ term is due to the symmetry of the grand resistance matrix, which requires that the degenerate quadrupole induced by a sphere in a uniform flow is the same as the Stokeslet induced by a degenerate quadratic velocity field. The velocity and traction at the particle surface can be obtained with straightforward algebra,

$$\begin{aligned} u_i \;=\; & \left(1 - \frac{f_1 + 2f_2}{6}\right)\langle u_i\rangle - \frac{f_1 - 6f_2}{6} n_i n_j \langle u_j\rangle + \left(1 - \frac{2\ell_1}{3}\right)\varepsilon_{ijk}\langle\omega_j\rangle r_k \\ & + (1 - 2s_2)\,\langle e_{ij}\rangle r_j - (s_1 - 5s_2) r_i \langle e_{jk}\rangle n_j n_k + \left(\frac{1}{2} + q_1^I - 30 q_2^I\right)\langle u_{\{i,jk\}}\rangle r_j r_k \\ & - 5\left(q_1^I - 14 q_2^I\right) n_i n_j \langle u_{\{j,k\ell\}}\rangle r_k r_\ell - \left(1 - q_1^R\right)\frac{2\varepsilon_{ijk} r_j \langle\omega_{\{k,\ell\}}\rangle r_\ell}{3} \\ & + \left(2 - \frac{5}{3} f_2 - q_1^D\right)\frac{r^2\langle u_{i,jj}\rangle}{10} - \left(1 + \frac{5}{3} f_2 - 3 q_1^D\right)\frac{r_i r_j \langle u_{j,kk}\rangle}{10}. \end{aligned} \tag{D 3a}$$

$$\begin{aligned} \sigma_{ij} n_j \;=\; & \eta\frac{2f_2}{a}\langle u_i\rangle + \eta\frac{f_1 - 6f_2}{a} n_i n_j \langle u_j\rangle + 2\eta\ell_1\varepsilon_{ijk} n_k\langle\omega_j\rangle + 2\eta\,(1 - s_1 + 8s_2)\,\langle e_{ij}\rangle n_j \\ & + 8\eta(s_1 - 5s_2) n_i\langle e_{jk}\rangle n_j n_k - 2\eta\left(1 - 2\left(4q_1^I - 75 q_2^I\right)\right)\langle u_{\{i,jk\}}\rangle n_j n_k \\ & + 50\eta\left(q_1^I - 14 q_2^I\right) n_i n_j \langle u_{\{j,k\ell\}}\rangle n_k r_\ell - \left(1 + 4q_1^R\right)\frac{2\eta\varepsilon_{ijk} n_j\langle\omega_{\{k,\ell\}}\rangle r_\ell}{3} \\ & + (1 + 2q_1^D)\frac{3\eta r\langle u_{i,jj}\rangle}{10} - \left(3 + 6q_1^D - \frac{10}{3} f_2\right)\frac{3\eta n_i r_j\langle u_{j,kk}\rangle}{10}. \end{aligned} \tag{D 3b}$$

Substitution of the hydrodynamic velocity and traction into (3.14)–(3.17) yields terms corresponding to the upper right half of (4.5),

$$F_i^H = \frac{4\pi\eta a}{3}(f_1 + a^2 f_2\nabla^2)\langle u_i\rangle, \tag{D 4a}$$

$$D_{ij}^H = \frac{8\pi\eta a^3}{3}\left(\left(s_1 + \frac{a^2 s_2}{2}\nabla^2\right)\langle e_{ij}\rangle - \varepsilon_{ijk}\left(\ell_1 + \frac{a^2(5\ell_1 - 3)}{30}\nabla^2\right)\langle\omega_k\rangle\right), \tag{D 4b}$$

$$Q_{ijk}^H = \frac{8\pi\eta a^5}{3}\left(q_1^I\langle u_{\{i,jk\}}\rangle + \frac{q_1^R}{3}\left(\varepsilon_{kj\ell}\langle\omega_{\{\ell,i\}}\rangle + \varepsilon_{ki\ell}\langle\omega_{\{\ell,j\}}\rangle\right) + \frac{3q_1^D}{10}\Delta_{ijk\ell}^{(2,2)}\langle u_{\ell,mm}\rangle\right), \tag{D 4c}$$

where we have employed the generalized Faxén laws (B. E. Dolata and R. N. Zia, personal communication 2019) to compute the finite-size corrections to the stresslet and torque. The finite-size correction from the shear-rate Laplacian is well known, while the torque correction was obtained from a Taylor expansion of the Faxén torque operator,

$$L_i^H(\boldsymbol{x}) = \int\left(u_j^\infty 2\eta\ell_1\varepsilon_{jik} n_k - \sigma_{jk}^\infty\left(1 - \frac{2\ell_1}{3}\right)\varepsilon_{ji\ell} r_\ell n_k\right)\mathrm{d}S. \tag{D 5}$$

The resistance tensors in (4.5) are then obtained by recognizing that $\omega_i = \varepsilon_{ijk}u_{k,j}$, $\omega_{\{i,j\}} = \Delta_{ijnok\ell}^{(2,1,2)}\varepsilon_{nop}e_{k\ell,p}$ and $u_{i,jj} = 2\Delta_{jk\ell i}^{(2,2)} e_{jk,\ell}$.

https://doi.org/10.1017/jfm.2020.6 Published online by Cambridge University Press

The explicit values of the coefficients in the multipole solution to the Stokes equations can be inferred from prior results in the literature. Velocity field solutions for droplets, as given by the boundary conditions (4.18*a-c*), were computed by Rybczynski (1911) and Hadamard (1911) for translating spheres, Taylor (1932) for a shearing flow and by Nadim & Stone (1991) for a general quadratic flow. Prior results claiming no torque on a viscous droplet (Hetsroni & Haber 1970) are incorrect as they do not correctly account for the angular momentum balance in the boundary conditions. Solutions for slip spheres with boundary condition (4.20) were given for translating spheres by Basset (1888), while solutions rotating spheres and spheres in a shearing flow were given by Felderhof (1976). We are unaware of a prior solution for a Navier-slip sphere in a general quadratic flow.

REFERENCES

AGACY, R. L. 1999 Generalized Kronecker and permanent deltas, their spinor and tensor equivalents and applications. *J. Math. Phys.* **40** (4), 2055–2063.

AKSEL, N. 2002 A brief note from the editor on the 'second-order fluid'. *Acta Mech.* **157** (1), 235–236.

ANDERSON, T. B. & JACKSON, R. 1967 Fluid mechanical description of fluidized beds. Equations of motion. *Ind. Engng Chem. Fundam.* **6** (4), 527–539.

ASKES, H. & AIFANTIS, E. C. 2011 Gradient elasticity in statics and dynamics: an overview of formulations, length scale identification procedures, finite element implementations and new results. *Intl J. Solids Struct.* **48** (13), 1962–1990.

AUFFRAY, N. 2013 Geometrical picture of third-order tensors. In *Generalized Continua as Models for Materials*, pp. 17–40. Springer.

BASSET, A. B. 1888 *A Treatise on Hydrodynamics: with Numerous Examples*, vol. 2. Deighton, Bell and Company.

BATCHELOR, G. K. 1970 The stress system in a suspension of force-free particles. *J. Fluid Mech.* **41** (03), 545–570.

BATCHELOR, G. K. 1972 Sedimentation in a dilute dispersion of spheres. *J. Fluid Mech.* **52** (02), 245–268.

BATCHELOR, G. K. 1977 The effect of Brownian motion on the bulk stress in a suspension of spherical particles. *J. Fluid Mech.* **83** (01), 97–117.

BATCHELOR, G. K. & GREEN, J. T. 1972*a* The hydrodynamic interaction of two small freely-moving spheres in a linear flow field. *J. Fluid Mech.* **56** (02), 375–400.

BATCHELOR, G. K. & VAN RENSBURG, R. W. J. 1986 Structure formation in bidisperse sedimentation. *J. Fluid Mech.* **166**, 379–407.

BATCHELOR, G. K. & GREEN, J. T. 1972*b* The determination of the bulk stress in a suspension of spherical particles to order c^2. *J. Fluid Mech.* **56** (3), 401–427.

BERGOUGNOUX, L., GHICINI, S., GUAZZELLI, E. & HINCH, J. 2003 Spreading fronts and fluctuations in sedimentation. *Phys. Fluids* **15** (7), 1875–1887.

BERRET, J.-F. 2006 Rheology of wormlike micelles: equilibrium properties and shear banding transitions. In *Molecular Gels*, pp. 667–720. Springer.

BLEUSTEIN, J. L. & GREEN, A. E. 1967 Dipolar fluids. *Intl J. Engng Sci.* **5** (4), 323–340.

BRENNER, H. & HABER, S. 1984 Symbolic operator solutions of Laplace's and Stoke's equations Part I Laplace's equation. *Chem. Engng Commun.* **27** (5–6), 283–295.

BRUNN, P. 1980 Faxen relations of arbitrary order and their application. *Z. Angew. Math. Phys.* **31** (3), 332–343.

CHANG, C. S. & GAO, J. 1995 Second-gradient constitutive theory for granular material with random packing structure. *Intl J. Solids Struct.* **32** (16), 2279–2293.

COOPE, J. A. R. 1970 Irreducible Cartesian tensors. III. Clebsch–Gordan reduction. *J. Math. Phys.* **11** (5), 1591–1612.

https://doi.org/10.1017/jfm.2020.6 Published online by Cambridge University Press

DHONT, J. K. G. 1999 A constitutive relation describing the shear-banding transition. *Phys. Rev.* E **60** (4), 4534.

DHONT, J. K. G. & BRIELS, W. J. 2002 Stresses in inhomogeneous suspensions. *J. Chem. Phys.* **117** (8), 3992–3999.

DOMBROWSKI, C., CISNEROS, L., CHATKAEW, S., GOLDSTEIN, R. E. & KESSLER, J. O. 2004 Self-concentration and large-scale coherence in bacterial dynamics. *Phys. Rev. Lett.* **93** (9), 098103.

DUNKEL, J., HEIDENREICH, S., BÄR, M. & GOLDSTEIN, R. E. 2013 Minimal continuum theories of structure formation in dense active fluids. *New J. Phys.* **15** (4), 045016.

EHRENTRAUT, H. & MUSCHIK, W. 1998 On symmetric irreducible tensors in d-dimensions. *ARI Intl J. Phys. Engng Sci.* **51** (2), 149–159.

EINSTEIN, A. 1906 Eine neue bestimmung der moleküldimension. *Ann. Phys.* **19**, 289–306.

EINSTEIN, A. 1911 Berichtigung zu meiner arbeit: Eine neue bestimmung der moleküldimensionen. *Ann. Phys.* **339** (3), 591–592.

ERINGEN, A. C. 1966 Theory of micropolar fluids. *J. Math. Mech.* **16**, 1–18.

FELDERHOF, B. U. 1976 Force density induced on a sphere in linear hydrodynamics: II. Moving sphere, mixed boundary conditions. *Physica* A **84** (3), 569–576.

FRANK, M., ANDERSON, D., WEEKS, E. R. & MORRIS, J. F. 2003 Particle migration in pressure-driven flow of a Brownian suspension. *J. Fluid Mech.* **493**, 363–378.

GAO, T., HU, H. H. & CASTAÑEDA, P. P. 2011 Rheology of a suspension of elastic particles in a viscous shear flow. *J. Fluid Mech.* **687**, 209–237.

GRAD, H. 1952 Statistical mechanics, thermodynamics, and fluid dynamics of systems with an arbitrary number of integrals. *Commun. Pure Appl. Maths* **5** (4), 455–494.

HABER, S. & BRENNER, H. 1984 Symbolic operator solutions of Laplace's and Stoke's equations Part II Stokes flow past a rigid sphere. *Chem. Engng Commun.* **27** (5–6), 297–311.

HADAMARD, J. S. 1911 Mouvement permanent lent d'une sphère liquide et visqueuse dans un liquide visqueux. *C. R. Acad. Sci. Paris* **152**, 1735–1752.

HALSEY, T. C. 1992 Electrorheological fluids. *Science* **258** (5083), 761–766.

HALSEY, T. C. & TOOR, W. 1990 Structure of electrorheological fluids. *Phys. Rev. Lett.* **65** (22), 2820.

HEMINGWAY, E. J. & FIELDING, S. M. 2018 Edge-induced shear banding in entangled polymeric fluids. *Phys. Rev. Lett.* **120** (13), 138002.

HETSRONI, G. & HABER, S. 1970 The flow in and around a droplet or bubble submerged in an unbound arbitrary velocity field. *Rheol. Acta* **9** (4), 488–496.

JACKSON, R. 1997 Locally averaged equations of motion for a mixture of identical spherical particles and a Newtonian fluid. *Chem. Engng Sci.* **52** (15), 2457–2469.

JAKATA, K. & EVERY, A. G. 2008 Determination of the dispersive elastic constants of the cubic crystals Ge, Si, GaAs, and InSb. *Phys. Rev.* B **77** (17), 174301.

JEFFREY, D. J. 1973 Conduction through a random suspension of spheres. *Proc. R. Soc. Lond.* A **335**, 355–367.

JIN, H., KANG, K., AHN, K. H., BRIELS, W. J. & DHONT, J. K. G. 2018 Non-local stresses in highly non-uniformly flowing suspensions: the shear-curvature viscosity. *J. Chem. Phys.* **149** (1), 014903.

KIRCHHOFF, G. R. 1876 *Vorlesungen über Mathematische Physik: Mechanik*, vol. 1. Teubner.

KOH, C. J., HOOKHAM, P. & LEAL, L. G. 1994 An experimental investigation of concentrated suspension flows in a rectangular channel. *J. Fluid Mech.* **266**, 1–32.

LADYZHENSKAYA, O. A. 1969 *The Mathematical Theory of Viscous Incompressible Flow*, vol. 2. Gordon and Breach.

LEIGHTON, D. & ACRIVOS, A. 1987 The shear-induced migration of particles in concentrated suspensions. *J. Fluid Mech.* **181**, 415–439.

LHUILLIER, D. 1992 Ensemble averaging in slightly non-uniform suspensions. *Eur. J. Mech. (*B*/Fluids)* **11** (6), 649–661.

LYON, M. K. & LEAL, L. G. 1998*a* An experimental study of the motion of concentrated suspensions in two-dimensional channel flow. Part 1. Monodisperse systems. *J. Fluid Mech.* **363**, 25–56.

https://doi.org/10.1017/jfm.2020.6 Published online by Cambridge University Press

LYON, M. K. & LEAL, L. G. 1998*b* An experimental study of the motion of concentrated suspensions in two-dimensional channel flow. Part 2. Bidisperse systems. *J. Fluid Mech.* **363**, 57–77.

MARANGANTI, R. & SHARMA, P. 2007 A novel atomistic approach to determine strain-gradient elasticity constants: tabulation and comparison for various metals, semiconductors, silica, polymers and the (ir) relevance for nanotechnologies. *J. Mech. Phys. Solids* **55** (9), 1823–1852.

MASSELON, C., SALMON, J.-B. & COLIN, A. 2008 Nonlocal effects in flows of wormlike micellar solutions. *Phys. Rev. Lett.* **100** (3), 038301.

NADIM, A. 1996 A concise introduction to surface rheology with application to dilute emulsions of viscous drops. *Chem. Engng Commun.* **148** (1), 391–407.

NADIM, A. & STONE, H. A. 1991 The motion of small particles and droplets in quadratic flows. *Stud. Appl. Maths* **85** (1), 53–73.

O'BRIEN, R. W. 1979 A method for the calculation of the effective transport properties of suspensions of interacting particles. *J. Fluid Mech.* **91** (01), 17–39.

OLMSTED, P. D. 2008 Perspectives on shear banding in complex fluids. *Rheol. Acta* **47** (3), 283–300.

PARMAR, M., HASELBACHER, A. & BALACHANDAR, S. 2012 Equation of motion for a sphere in non-uniform compressible flows. *J. Fluid Mech.* **699**, 352–375.

PROSPERETTI, A. 2004 The average stress in incompressible disperse flow. *Intl J. Multiphase Flow* **30** (7–8), 1011–1036.

PROSPERETTI, A., ZHANG, Q. & ICHIKI, K. 2006 The stress system in a suspension of heavy particles: antisymmetric contribution. *J. Fluid Mech.* **554**, 125–146.

RAJA, R. V., SUBRAMANIAN, G. & KOCH, D. L. 2010 Inertial effects on the rheology of a dilute emulsion. *J. Fluid Mech.* **646**, 255–296.

RAMASWAMY, M., LIN, N. Y. C., LEAHY, B. D., NESS, C., FIORE, A. M., SWAN, J. W. & COHEN, I. 2017 How confinement-induced structures alter the contribution of hydrodynamic and short-ranged repulsion forces to the viscosity of colloidal suspensions. *Phys. Rev. X* **7** (4), 041005.

RAMKISSOON, H. & MAJUMDAR, S. R. 1976 Representations and fundamental singular solutions in micropolar fluid. *Z. Angew. Math. Mech.* **56** (5), 197–203.

RYBCZYNSKI, W. 1911 On the translatory motion of a fluid sphere in a viscous medium. *Bull. Acad. Sci., Cracow* A 40–46.

SEGRE, G. & SILBERBERG, A. 1961 Radial particle displacements in Poiseuille flow of suspensions. *Nature* **189** (4760), 209–210.

SŁOMKA, J. & DUNKEL, J. 2017 Geometry-dependent viscosity reduction in sheared active fluids. *Phys. Rev. Fluids* **2** (4), 043102.

SONN-SEGEV, A., BERNHEIM-GROSWASSER, A., DIAMANT, H. & ROICHMAN, Y. 2014 Viscoelastic response of a complex fluid at intermediate distances. *Phys. Rev. Lett.* **112** (8), 088301.

STOKES, G. G. 1851 *On the Effect of the Internal Friction of Fluids on the Motion of Pendulums*, vol. 9. Pitt Press Cambridge.

STOKES, V. K. 1966 Couple stresses in fluids. *Phys. Fluids* **9** (9), 1709–1715.

STRATING, P. 1995 The stress tensor in colloidal suspensions. *J. Chem. Phys.* **103** (23), 10226–10237.

SWAN, J. W. & BRADY, J. F. 2011 The hydrodynamics of confined dispersions. *J. Fluid Mech.* **687**, 254–299.

TAYLOR, G. I. 1932 The viscosity of a fluid containing small drops of another fluid. *Proc. R. Soc. Lond.* A **138** (834), 41–48.

TEE, S., MUCHA, P. J., CIPELLETTI, L., MANLEY, S., BRENNER, M. P., SEGRE, P. N. & WEITZ, D. A. 2002 Nonuniversal velocity fluctuations of sedimenting particles. *Phys. Rev. Lett.* **89** (5), 054501.

TIRUMKUDULU, M., MILEO, A. & ACRIVOS, A. 2000 Particle segregation in monodisperse sheared suspensions in a partially filled rotating horizontal cylinder. *Phys. Fluids* **12** (6), 1615–1618.

WHITMORE, R. L. 1955 The sedimentation of suspensions of spheres. *Brit. J. Appl. Phys.* **6** (7), 239–245.

WILEMSKI, G. 1976 On the derivation of Smoluchowski equations with corrections in the classical theory of Brownian motion. *J. Stat. Phys.* **14** (2), 153–169.

https://doi.org/10.1017/jfm.2020.6 Published online by Cambridge University Press

WOLGEMUTH, C. W. 2008 Collective swimming and the dynamics of bacterial turbulence. *Biophys. J.* **95** (4), 1564–1574.

ZAKHARI, M. E. A., ANDERSON, P. D. & HÜTTER, M. 2018 Modeling the shape dynamics of suspensions of permeable ellipsoidal particles. *J. Non-Newtonian Fluid Mech.* **259**, 23–31.

ZHANG, D. Z. & PROSPERETTI, A. 1994*a* Averaged equations for inviscid disperse two-phase flow. *J. Fluid Mech.* **267**, 185–219.

ZHANG, D. Z. & PROSPERETTI, A. 1994*b* Ensemble phase-averaged equations for bubbly flows. *Phys. Fluids* **6** (9), 2956–2970.

ZHANG, D. Z. & PROSPERETTI, A. 1997 Momentum and energy equations for disperse two-phase flows and their closure for dilute suspensions. *Intl J. Multiphase Flow* **23** (3), 425–453.

ZHOU, G. & PROSPERETTI, A. 2020 Lamb's solution and the stress moments for a sphere in Stokes flow. *Eur. J. Mech. (B/Fluids)* **79**, 270–282.

ZOU, W.-N., ZHENG, Q.-S., DU, D.-X. & RYCHLEWSKI, J. 2001 Orthogonal irreducible decompositions of tensors of high orders. *Math. Mech. Solids* **6** (3), 249–267.

https://doi.org/10.1017/jfm.2020.6 Published online by Cambridge University Press